tic adrenocortex in patients with aldosteronoma (2, 31). Previous *in vitro* studies demonstrated that Nurr1 and/or NGFI-B were rapidly induced by various factors, including ACTH (32) and angiotensin II (14). However, unexpectedly, Nurr1 and NGFI-B immunoreactivities in the attached nonneoplastic adrenal cortex of adenoma were not significantly different from those in the nonpathological adrenal cortex in our study. It is difficult to explain the mechanisms of these findings, but Davis and Lau (32) reported that NGFI-B isolated from ACTH-stimulated Y-1 cells was hypophosphorylated at serine 354 and significantly bound to its responsive element, whereas NGFI-B present in the unstimulated cells did not. The expression of Nurr1 or NGFI-B was generally considered to be regulated by multiple pathways, and the transcriptional activity is intricately modulated by phosphorylation (24). Therefore, a decrement in steroidogenesis in the attached nonneoplastic adrenal cortex of an adenoma may be partly due to the changes in posttranslational modifications of Nurr1 and/or NGFI-B. Additional examinations are required to clarify this hypothesis.

Acknowledgments

We appreciate the assistance of Ms. Chika Kaneko and Mr. Katsuhiko Ono (Department of Pathology, Tohoku University School of Medicine, respectively) for their skillful technical assistance.

Received January 14, 2004. Accepted May 5, 2004.

Address all correspondence and requests for reprints to: Dr. Takashi Suzuki, Department of Pathology, Tohoku University School of Medicine, 2-1 Seiryo-machi, Aoba-ku, Sendai 980-8575, Japan. E-mail: t-suzuki@patholo2.med.tohoku.ac.jp.

This work was supported in part by NIH Grant DK-43140 (to W.E.R.).

References

1. **Neville AM, O'Hare MJ** 1982 Functional activity of the adrenal cortex. In: The human adrenal cortex. New York: Springer-Verlag; 68–98
2. **Sasano H** 1994 Localization of steroidogenic enzymes in adrenal cortex and its disorders. Endocr J 41:471–482
3. **Ogishima T, Shibata H, Shimada H, Mitani F, Suzuki H, Saruta T, Ishimura Y** 1991 Aldosterone synthase cytochrome P-450 expressed in the adrenals of patients with primary aldosteronism. J Biol Chem 266:10731–10734
4. **Ogo A, Haji M, Ohashi M, Nawata H** 1991 Markedly increased expression of cytochrome P-450 17α-hydroxylase (P-450c17) mRNA in adrenocortical adenomas from patients with Cushing's syndrome. Mol Cell Endocrinol 80:83–89
5. **Suzuki T, Sasano H, Sawai T, Tsunoda K, Nisikawa T, Abe K, Yoshinaga K, Nagura H** 1992 Small adrenocortical tumors without apparent clinical endocrine abnormalities. Immunolocalization of steroidogenic enzymes. Pathol Res Pract 188:883–889
6. **Giguere V** 1999 Orphan nuclear receptors: from gene to function. Endocr Rev 20:689–725
7. **Davis IJ, Hazel TG, Lau LF** 1991 Transcriptional activation by Nur77, a growth factor-inducible member of the steroid hormone receptor superfamily. Mol Endocrinol 5:854–859
8. **Wilson TE, Fahrner TJ, Johnston M, Milbrandt J** 1991 Identification of the DNA binding site for NGFI-B by genetic selection in yeast. Science 252:1296–1300
9. **Saucedo-Cardenas O, Quintana-Hau JD, Le WD, Smidt MP, Cox JJ, De Mayo F, Burbach JP, Conneely OM** 1998 Nurr1 is essential for the induction of the dopaminergic phenotype and the survival of ventral mesencephalic late dopaminergic precursor neurons. Proc Natl Acad Sci USA 95:4013–4018
10. **Milbrandt J** 1998 Nerve growth factor induces a gene homologous to the glucocorticoid receptor gene. Neuron 1:183–188
11. **Lee SL, Wesselschmidt RL, Linette GP, Kanagawa O, Russell JH, Milbrandt J** 1995 Unimpaired thymic and peripheral T cell death in mice lacking the nuclear receptor NGFI-B (Nur77). Science 269:532–535
12. **Perlmann T, Jansson L** 1995 A novel pathway for vitamin A signaling mediated by RXR heterodimerization with NGFI-B and NURR1. Genes Dev 9:769–782
13. **Davis IJ, Lau LF** 1994 Endocrine and neurogenic regulation of the orphan nuclear receptors Nur77 and Nurr-1 in the adrenal glands. Mol Cell Biol 14:3469–3483
14. **Bassett M, Suzuki T, Sasano H, White PC, Rainey WE** 2004 A role for the NGFIB family of transactivation factors in adrenal aldosterone production. Mol Endocrinol 18:279–290
15. **Weiss LM** 1984 Comparative histologic study of 43 metastasizing and nonmetastasizing adrenocortical tumors. Am J Surg Pathol 8:163–169
16. **McCarty Jr KS, Miller LS, Cox EB, Konrath J, McCarty KS Sr** 1985 Estrogen receptor analyses. Correlation of biochemical and immunohistochemical methods using monoclonal antireceptor antibodies. Arch Pathol Lab Med 109:716–721
17. **Suzuki T, Takahashi K, Darnel AD, Moriya T, Murakami O, Narasaka T, Takeyama J, Sasano H** 2000 COUP-TFII in the human adrenal cortex and its disorders. J Clin Endocrinol Metab 85:2752–2757
18. **Dumoulin FL, Nischalke HD, Leifeld L, von dem Bussche A, Rockstroh JK, Sauerbruch T, Spengler U** 2000 Semi-quantification of human C-C chemokine mRNAs with reverse transcription/real-time PCR using multi-specific standards. J Immunol Methods 241:109–119
19. **Maruyama K, Tsukada T, Bandoh S, Sasaki K, Ohkura N, Yamaguchi K** 1995 Expression of NOR-1 and its closely related members of the steroid/thyroid hormone receptor superfamily in human neuroblastoma cell lines. Cancer Lett 96:117–122
20. **Wilson TE, Mouw AR, Weaver CA, Milbrandt J, Parker KL** 1993 The orphan nuclear receptor NGFI-B regulates expression of the gene encoding steroid 21-hydroxylase. Mol Cell Biol 13:861–868
21. **Yoshimura M, Nakamura S, Ito T, Nakayama M, Harada E, Mizuno Y, Sakamoto T, Yamamuro M, Saito Y, Nakao K, Yasue H, Ogawa H** 2002 Expression of aldosterone synthase gene in failing human heart: quantitative analysis using modified real-time polymerase chain reaction. J Clin Endocrinol Metab 87:3936–3940
22. **Suzuki T, Nakata T, Miki Y, Kaneko C, Moriya T, Ishida T, Akinaga S, Hirakawa H, Kimura M, Sasano H** 2003 Estrogen sulfotransferase and steroid sulfatase in human breast carcinoma. Cancer Res 63:2762–2770
23. **Rainey WE** 1999 Adrenal zonation: clues from 11β-hydroxylase and aldosterone synthase. Mol Cell Endocrinol 151:151–160
24. **Nordzell M, Aarnisalo P, Benoit G, Castro DS, Perlmann T** 2004 Defining an N-terminal activation domain of the orphan nuclear receptor Nurr1. Biochem Biophys Res Commun 313:205–211
25. **Chang SF, Chung BC** 1995 Difference in transcriptional activity of two homologous CYP21A genes. Mol Endocrinol 9:1330–1336
26. **Bassett MH, Jimemez PT, Carr BR, Rainey WE,** Transcriptional regulation of 3β-hydroxysteroid dehydrogenase type 2 (3βHSD2) by the transcription factor NGFIB (NR4A1). Proc of the 84th Annual Meeting of The Endocrine Society, San Francisco, CA, 2002, p 342 (Abstract P2–86)
27. **Suzuki T, Sasano H, Takeyama J, Kaneko C, Freije WA, Carr BR, Rainey WE** 2000 Developmental changes in steroidogenic enzymes in human postnatal adrenal cortex: immunohistochemical studies. Clin Endocrinol (Oxf) 53: 739–747
28. **Narasaka T, Suzuki T, Moriya T, Sasano H** 2001 Temporal and spatial distribution of corticosteroidogenic enzymes immunoreactivity in developing human adrenal. Mol Cell Endocrinol 174:111–120
29. **Mesiano S, Jaffe RB** 1997 Developmental and functional biology of the primate fetal adrenal cortex. Endocr Rev 18:378–403
30. **Rainey WE, Carr BR, Wang ZN, Parker Jr CR** 2001 Gene profiling of human fetal and adult adrenals. J Endocrinol 171:209–215
31. **Sasano H, White PC, New MI, Sasano N** 1988 Immunohistochemical localization of cytochrome P-450C21 in human adrenal cortex and its relation to endocrine function. Hum Pathol 19:181–185
32. **Davis IJ, Lau LF** 1994 Endocrine and neurogenic regulation of the orphan nuclear receptors Nur77 and Nurr-1 in the adrenal glands. Mol Cell Biol 14:3469–3483

JCEM is published monthly by The Endocrine Society (http://www.endo-society.org), the foremost professional society serving the endocrine community.

Pediatric Neurosurgery

Pediatr Neurosurg 2004;40:149–150
DOI: 10.1159/000079862

High-Grade Spinal Cord Tumor with Cerebellar and Retroperitoneal Extension

Kazuyoshi Morimoto Akatsuki Wakayama Toshiki Yoshimine
Masahiro Nakayama

Osaka Medical Center and Research Institute for Maternal and Child Health, Osaka, Japan

A 4-month-old girl presented with a 3-week history of fecal incontinence and a 1-week history of paraparesis. She exhibited no voluntary motion of the lower extremities.

Spinal magnetic resonance imaging revealed an intradural intramedullary mass under the T9 region that exhibited a swelling cord with an area of high intensity on T1-weighted imaging (fig. 1a).

A preoperative brain CT scan 2 weeks later revealed another multiple cerebellar enhanced lesion, although the initial CT scan had not revealed any lesion (fig. 1B). The patient underwent laminotomy and posterior fossa craniectomy, and then partial excision of the spinal and cerebellar tumors. Examination of formalin-fixed, paraffin-embedded sections of the cerebellar masses showed poorly differentiated, pleomorphic cells with marked nuclear atypia and brisk mitotic activity (fig. 1C). However, the histology of the spinal tumor was not verified. Although craniospinal irradiation (50 Gy) in addition to chemotherapy was performed for 3 months, abdominal and back distension appeared. An axial body CT scan revealed an enormous retroperitoneal extension (fig. 1D). She died 2 weeks later. At autopsy, the spinal cord tumor was found to extend through the intervertebral foramen to the retro-

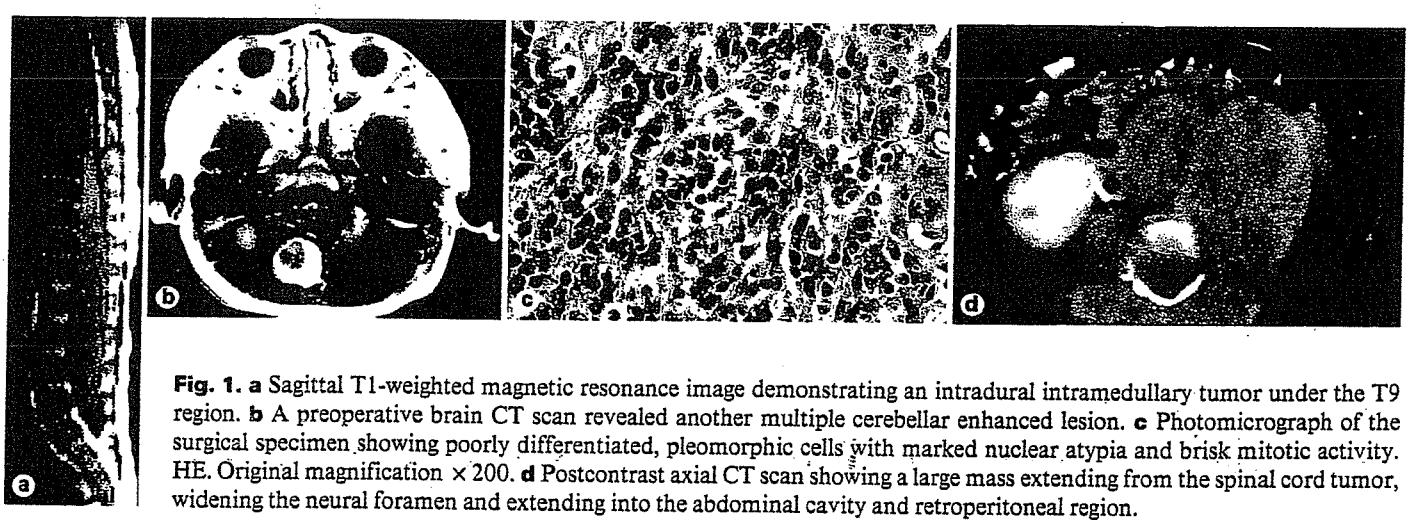

Fig. 1. a Sagittal T1-weighted magnetic resonance image demonstrating an intradural intramedullary tumor under the T9 region. **b** A preoperative brain CT scan revealed another multiple cerebellar enhanced lesion. **c** Photomicrograph of the surgical specimen showing poorly differentiated, pleomorphic cells with marked nuclear atypia and brisk mitotic activity. HE. Original magnification × 200. **d** Postcontrast axial CT scan showing a large mass extending from the spinal cord tumor, widening the neural foramen and extending into the abdominal cavity and retroperitoneal region.

KARGER
Fax +41 61 306 12 34
E-Mail karger@karger.ch
www.karger.com

1016–2291/04/0403–0149$21.00/0

Accessible online at:
www.karger.com/pne

K. Morimoto, MD
Department of Neurosurgery
Osaka Medical Center and Research Institute for Maternal and Child Health
Izumi, Osaka 594-1101 (Japan)
Tel. +81 725 56 1220, Fax +81 725 56 5682, E-Mail fr8kmrmt@mch.pref.osaka.jp

peritoneal region. Although the spinal cord tumor also showed the histology of a positive component with PTAH staining, the retroperitoneal tumor specimen contained rhabdoid cells which were positive on immunostaining for vimentin and epithelial membrane antigen [1].

There have been relatively few reported experiences of high-grade spinal cord tumors in the pediatric population [2, 3]. Unfortunately, these tumors invariably progress despite aggressive chemotherapy and radiotherapy. This is a rare case of a high-grade spinal cord tumor with cerebellar and retroperitoneal extension in a 4-month-old girl.

References

1 Rorke LB, Packer RJ, Biegel JA: Central nervous system atypical teratoid/rhabdoid tumors of infancy and childhood: Definition of an entity. J Neurosurg 1996;85:56–65.

2 Constantini S, Houten J, Miller DC, Freed D, Ozek MM, Rorke LB, Allen JC, Epstein FJ: Intramedullary spinal cord tumors in children under the age of 3 years. J Neurosurg 1996;85:1036–1043.

3 Merchant TE, Nguyen D, Thompson SJ, Reardon DA, Kun LE, Sanford RA: High-grade pediatric spinal cord tumors. Pediatr Neurosurg 1999;30:1–5.

Int. J. Cancer: **112,** 219–224 (2004)

Publication of the International Union Against Cancer

FENRETINIDE INDUCES SUSTAINED-ACTIVATION OF JNK/p38 MAPK AND APOPTOSIS IN A REACTIVE OXYGEN SPECIES-DEPENDENT MANNER IN NEUROBLASTOMA CELLS

Shinya OSONE*, Hajime HOSOI, Yasumichi KUWAHARA, Yoshifumi MATSUMOTO, Tomoko IEHARA and Tohru SUGIMOTO

Department of Pediatrics, Kyoto Prefectural University of Medicine, Graduate School of Medical Science, Kyoto, Japan

Fenretinide, which mediates apoptosis in neuroblastoma cells, is being considered as a novel therapeutic for neuroblastoma. The cytotoxic mechanisms of fenretinide, however, have not been fully elucidated. Sustained-activation of JNK and p38 MAPK signaling has been shown recently to have a pivotal role in stress-induced apoptosis. Whether fenretinide activates the signaling in neuroblastoma cells is not known. In the present study, fenretinide induced sustained-activation of both JNK and p38 MAPK in neuroblastoma cells. Pretreatment with the antioxidant L-ascorbic acid almost completely inhibited the accumulation of fenretinide-induced intracellular reactive oxygen species (ROS), activation of JNK and p38 MAPK and apoptosis. Intracellular ROS production and activation of stress signaling was not altered by fenretinide in resistant neuroblastoma cells. Our study demonstrates that in neuroblastoma cells, fenretinide induces sustained-activation of JNK and p38 MAPK in an ROS-dependent manner and indicates that JNK and p38 MAPK signaling might mediate fenretinide-induced apoptosis. Our results also indicate that suppression of the fenretinide-induced ROS productive system and the downstream JNK and p38 MAPK signaling pathways causes neuroblastoma cells to become resistant to fenretinide.

Key words: *fenretinide; neuroblastoma; apoptosis; reactive oxygen species; JNK; p38 MAPK*

Neuroblastoma (NB) is one of the common malignant solid tumors in childhood, arising from neural crest progenitors. Despite progress with multimodal therapies consisting of multidrug chemotherapy, surgical and radiation therapy, the prognosis of advanced NB remains poor.[1] Therefore, new therapeutic approaches are needed. Retinoic acids (RA), which are vitamin A analogs, have been shown to induce the differentiation of NB cells into mature neuronal cells.[2] It has been reported recently that oral administration of 13-cis RA after consolidated chemotherapy with stem cell transplantation improved the 3-year event-free survival of advanced NB patients.[3] Retinoic acids are expected to be used as new therapeutic agents against NB, in view of their relatively low toxicity.

N-(4-hydroxyphenyl) retinamide, also called fenretinide (FR), has cytotoxic activity against various tumor cells including NB.[4] An advantage of FR is that its systemic toxicity is less than that of RA.[5,6] The cytotoxicity of FR is due mainly to its ability to induce apoptosis, although the mechanism has not been fully elucidated.[4] Several studies have shown that, in NB cell lines, FR produced intracellular reactive oxygen species (ROS).[7–9] In addition, FR increases intracellular ceramide, which is known as an inducer of apoptosis, in NB cells.[7,10,11]

Mitogen-activated protein kinases (MAPK) are well-conserved signaling proteins in eukaryotic cells and have essential roles in deciding cell fate.[12,13] Two members of the MAPK family, c-Jun N-terminal kinase (JNK) and p38 MAPK, are activated by various stress stimuli including oxidative stress and chemical agents.[12–14] When activated, they phosphorylate downstream transcription factors of c-Jun and activating transcription factor-2 (ATF-2). Sustained-activation of JNK and p38 MAPK induces cell death.[13,15]

In prostate carcinoma cell lines, FR did not activate p38 MAPK, but it did activate JNK in an ROS-independent manner,[16] and the JNK pathway mediated FR-induced apoptotic signaling.[16,17] It has also been shown that FR activated JNK in A431 epidermoid carcinoma cells.[18] It is not known, however, whether FR activates JNK and p38 MAPK signaling in NB cells, or whether signaling is essential for FR-induced apoptosis. We examined stress signaling and apoptosis induced by FR in NB cells. We found that FR induced sustained-activation of both JNK and p38 MAPK in NB cells, indicating that JNK and p38 MAPK mediate FR-induced apoptosis. We also examined the relationship between the FR-induced ROS generation and the JNK/p38 MAPK signaling, and found that their activation is ROS-dependent. Moreover, we demonstrated that FR failed to produce intracellular ROS and to activate the kinases in the resistant NB cells, indicating the suppression of FR-induced ROS production and activation of JNK/p38 MAPK is one of the mechanisms of resistance to FR in NB cells.

MATERIAL AND METHODS

Cell culture

Human NB cell lines KP-N-TK[19] and KP-N-SIFA[20] were cultured in RPMI 1640 containing penicillin (100 U/ml), streptomycin (100 μg/ml) and 10% heat-inactivated FBS at 37°C in a 5% CO_2 incubator. The medium was changed every 3–4 days. Cells were sub-cultured into new flasks by trypsinization when in a sub-confluent state. FR-resistant cells of KP-N-TK, designated as KP-N-TK (FR-R), were established by culturing parental KP-N-TK cells with increasing concentrations of FR from 0.5–5 μM for 150 days. The cells were then maintained continuously in 5 μM FR.

Antibodies and reagents

Polyclonal antibodies against JNK, p38 MAPK, Thr^{183}/Tyr^{185}-phosphorylated JNK, Thr^{180}/Tyr^{182}-phosphorylated p38 MAPK were purchased from Cell Signaling Technology (Beverly, MA). Monoclonal anti-caspase-3 antibody was from BD Biosciences (San Jose, CA). Monoclonal anti-caspase-9 and anti-poly (ADP-ribose) polymerase (PARP) antibodies were obtained from Oncogene Research Products (San Diego, CA). FR (Toronto Research

Abbreviations: AA, L-ascorbic acid; CM-H_2DCFDA, 5(-6)-chloromethyl-2′-7′-dichlorodihydrofluorescein diacetate; FR, fenretinide; JNK, c-Jun N-terminal kinase; NB, neuroblastoma; p38 MAPK, p38 mitogen-activated protein kinase; PARP, poly (ADP-ribose) polymerase; ROS, reactive oxygen species; TUNEL, TdT-mediated dUTP-biotin nick end labeling.

Grant sponsor: Ministry of Education, Culture, Sports, Science and Technology, Japan; Grant number: 14370250, 15659248, 15659249; Grant sponsor: Ministry of Health and Welfare, Japan; Grant number: 13-19.

*Correspondence to: Department of Pediatrics, Kyoto Prefectural University of Medicine, Graduate School of Medical Science. 465 Kajii-cho, Kamigyo-ku, Kyoto 602-8566, Japan. Fax: +81-75-252-1399.
E-mail: shinn-o@koto.kpu-m.ac.jp

Received 30 September 2003; Accepted 6 April 2004

DOI 10.1002/ijc.20412
Published online 10 June 2004 in Wiley InterScience (www.interscience.wiley.com).

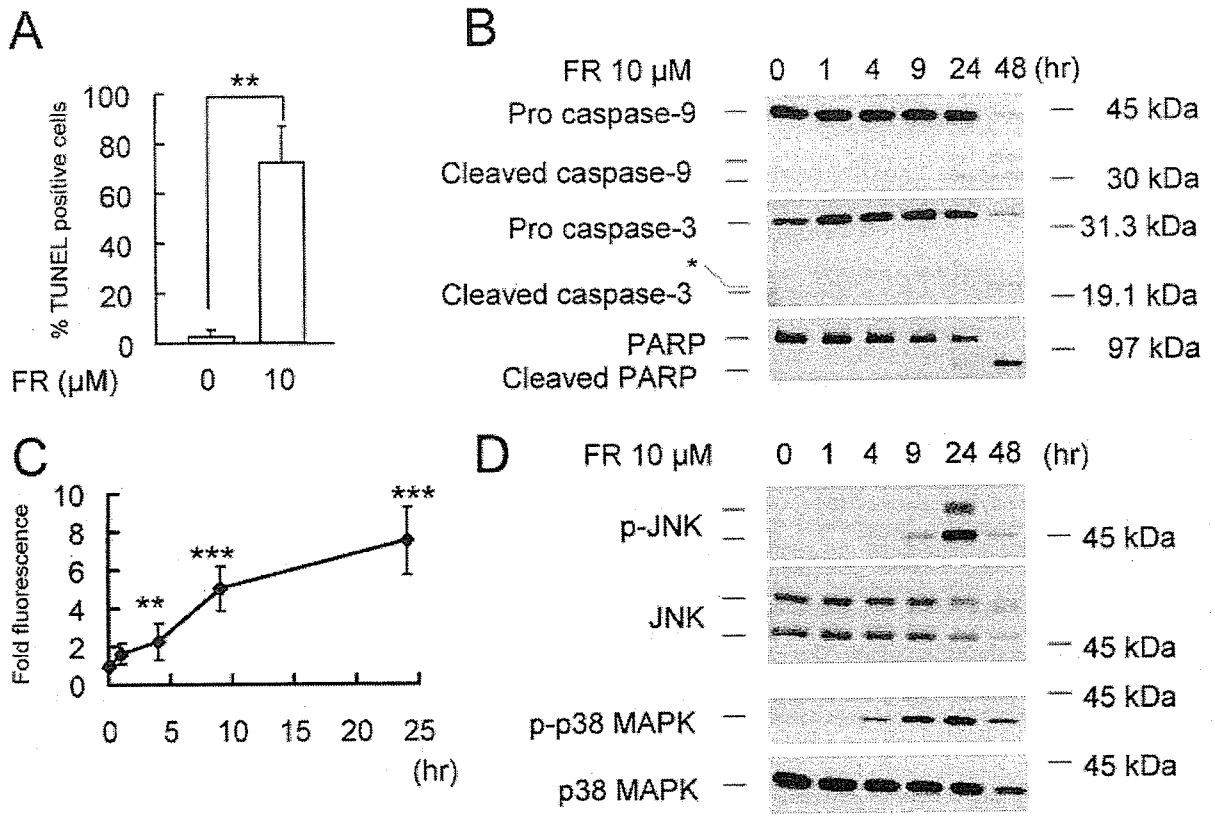

FIGURE 1 – Fenretinide-induced apoptosis, intracellular ROS accumulation and activation of JNK and p38 MAPK in KP-N-TK cells. (*a*) TUNEL assay. Cells were incubated with 10 μM FR or DMSO vehicle for 48 hr. Harvested cells were fixed as described in Material and Methods. After the TdT reaction with FITC labeling, cells were analyzed with a flow cytometer, and the percentage of TUNEL-positive cells was determined (mean + SD, $n = 3$). $^{**}p < 0.01$ (Student's *t*-test). (*b*) Time-course of cleavages of caspase-9, caspase-3 and PARP. Cells were treated with 10 μM FR for the times indicated. Lysates were prepared and immunoblotted for anti-caspase-9, anti-caspase-3 or anti-PARP antibodies. This is representative of 3 independent experiments. The band indicated by an asterisk is a non-specific band. (*c*) Time-course of intracellular ROS accumulation. Cells were incubated with 10 μM FR for the times indicated. CM-H_2DCFDA was added for 2 hr before cell harvesting. Flow cytometric analysis was carried out and the mean fluorescence was calculated (mean + SD, $n = 7$). $^{**}p < 0.01$, $^{***}p < 0.001$ (compared to control, Student's *t*-test) (*d*) Time-course of the activation of JNK and p38 MAPK. Cells were incubated with 10 μM FR for the times indicated. Immunoblotting was carried out using anti-phospho (p)-JNK, anti-JNK, anti-p-p38 MAPK or anti-p38 MAPK. This is representative of 3 independent experiments.

Chemicals, North York, Canada) was dissolved in dimethyl sulfoxide (DMSO) and stored at −70°C in the dark. L-Ascorbic acid (AA) (Wako Pure Chemical Ind., Osaka, Japan) was dissolved in distilled water and stored at −20°C. 5(-6)-Chloromethyl-2′-7′-dichlorodihydrofluorescein diacetate (CM-H_2DCFDA) (Molecular Probes, Eugene, OR) was freshly prepared in DMSO before use. The final concentration of DMSO was <0.2% in all experiments.

Western blotting

Cells (5×10^6) were seeded onto 100-mm dishes. When 50–60% confluence was achieved, cells were treated with 10 μM FR at 37°C with or without pretreatment of 400 μM AA for 12 hr. After the indicated periods, cells were washed once with ice-cold PBS. Floating cells were also collected. Cells were solubilized in RIPA buffer (150 mM NaCl, 50 mM Tris pH 8.0, 1% Nonidet P-40, 0.5% deoxycholate, 0.1% sodium dodecyl sulfate). Protein concentration was determined using a DC protein assay (Bio-Rad Laboratories, Hercules, CA). Cell lysates were electrophoresed on SDS-polyacrylamide gels, and then transferred to a PVDF membrane. The membrane was blocked in Tris-buffered saline (TBS) with 0.1% Tween 20 (TBS-T) and 5% nonfat skim milk, and subsequently probed with the primary antibody. The blots were washed in TBS-T and treated with the appropriate secondary antibodies (Amersham, Arlington, IL), and then analyzed using the ECL chemiluminescence system (Amersham).

Apoptosis assay

Apoptosis was determined using the MEBSTAIN Apoptosis Detection Kit Direct (Medical & Biological Laboratories Co., Nagoya, Japan) according to the manufacturer's protocol. In brief, cells (2×10^6) were plated onto 60-mm dishes. At 50–60% confluence, cells were treated with 10 μM FR at 37°C with or without preincubation with 400 μM AA for 12 hr. After 48 hr, cells were harvested, washed with PBS, and then fixed with 4% paraformaldehyde for 30 min at 4°C. Subsequently, cells were permeabilized with 70% ethanol for more than 30 min at −20°C, and incubated with the mixture of TdT and FITC-conjugated dUTP for 1 hr at 37°C. The cells were analyzed with a FACS Calibur flow cytometer (Nippon Becton Dickinson Co., Tokyo, Japan) and the number of the TUNEL (TdT-mediated dUTP-biotin nick end labeling)-positive cells was calculated using Cell Quest software (Nippon Becton Dickinson Co.).

The cleavages of caspase-9, caspase-3 and PARP were also detected by Western blotting as described above.

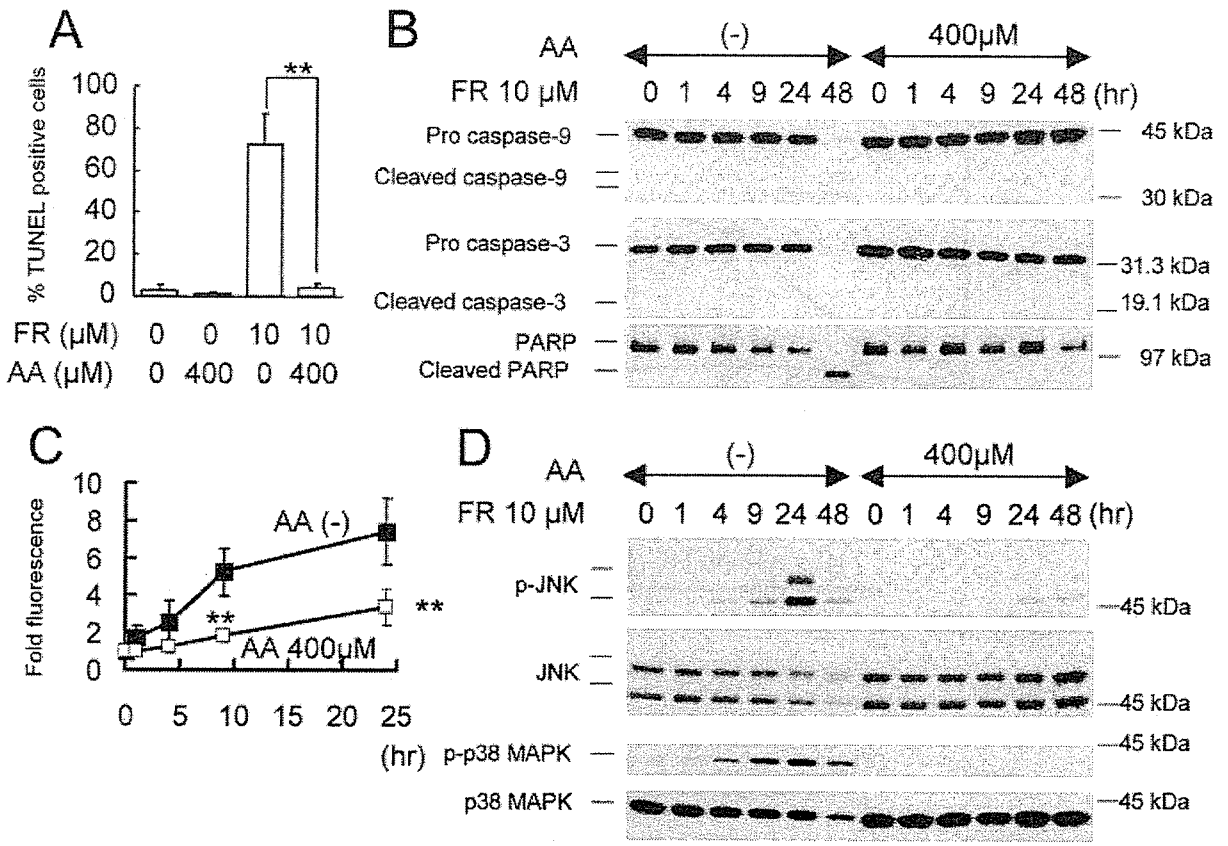

FIGURE 2 – L-Ascorbic acid (AA) inhibits FR-induced apoptosis, ROS accumulation and activation of JNK and p38 MAPK in KP-N-TK cells. Cells were treated with 10 μM FR with or without pretreatment with 400 μM AA for 12 hr. (*a*) TUNEL assay. Cells were incubated with FR or DMSO vehicle for 48 hr. TUNEL assay was carried out as described in Figure 1 (mean + SD, $n = 3$). $^{**}p < 0.01$ (Student's *t*-test). (*b*) Time-course of cleavages of caspase-9, caspase-3 and PARP. Cells were incubated with FR for the times indicated. Immunoblot analysis was carried out as described in Figure 1. This is representative of 3 independent experiments. (*c*) Time-course of intracellular ROS accumulation. Flow cytometric analysis using CM-H_2DCFDA was carried out as described in Figure 1 (mean + SD, $n = 4$). $^{**}p < 0.01$ (Student's *t*-test, compared to no pretreatment of AA). (*d*) Time-course of activation of JNK and p38 MAPK. Cells were incubated with FR for the times indicated with or without pretreatment with AA. Western blot analysis was carried out as described in Figure 1. This is representative of 3 independent experiments.

Determination of intracellular ROS

The intracellular concentration of ROS was measured using CM-H_2DCFDA as a probe. This probe is a non-polar compound that readily diffuses into cells, where it is hydrolyzed to the non-fluorescent polar derivative 2′,7′-dichlorofluorescin and thereby trapped within the cells. In the presence of a proper oxidant, 2′,7′-dichlorofluorescin is oxidized to highly fluorescent 2′,7′-dichlorofluorescein. Cells were plated onto 6-well dishes (5×10^5 cells /well) and treated with 10 μM FR with or without pretreatment of 400 μM AA as above. Two hours before cell harvest, 5 μM CM-H_2DCFDA was added to the cells. After the indicated periods, the medium was removed; cells were washed once with PBS, harvested, and suspended in PBS. The cells were immediately analyzed with a FACS Calibur flow cytometer; the excitation and emission wavelengths were at 488 nm and 530 nm, respectively. The mean fluorescence of 1×10^4 cells per sample was calculated using Cell Quest software.

RESULTS

Fenretinide induces apoptosis, intracellular ROS production and sustained-activation of JNK and p38 MAPK in KP-N-TK NB cells

We first studied FR-induced apoptosis in KP-N-TK cells. After 48 hr incubation with 10 μM FR, up to 70% of the cells were TUNEL-positive (Fig. 1*a*). The DMSO vehicle did not induce apoptosis (Fig. 1*a*). Cleavages of caspase-9, caspase-3 and PARP appeared 24 hr after the treatment, and progressed at 48 hr (Fig. 1*b*). We then studied the intracellular ROS production by FR in KP-N-TK cells. The fluorescence of CM-H_2DCFDA increased gradually during 24 hr of incubation with 10 μM FR (Fig. 1*c*). DMSO vehicle alone did not increase the fluorescence (data not shown).

Fenretinide induced sustained-activation of both JNK and p38 MAPK in KP-N-TK cells (Fig. 1*d*). The phosphorylation of JNK and p38 MAPK was observed from 4–48 hr after treatment with 10 μM FR, and peaked at 24 hr after treatment. The total amounts of JNK and p38 MAPK decreased at 48 hr. Short incubation with FR from 15 min (data not shown) and 1 hr (Fig. 1*d*) did not activate these kinases. The DMSO vehicle alone also did not alter their activation (data not shown).

L-Ascorbic acid suppresses fenretinide-induced apoptosis, intracellular ROS accumulation and activation of JNK and p38 MAPK

KP-N-TK cells were pretreated with 400 μM of the antioxidant AA and then incubated with 10 μM FR for 48 hr. Pretreatment with AA almost completely blocked FR-induced apoptosis (Fig. 2*a*). Fenretinide-induced processing of caspase-9, caspase-3 and PARP was also suppressed in the presence of AA (Fig. 2*b*).

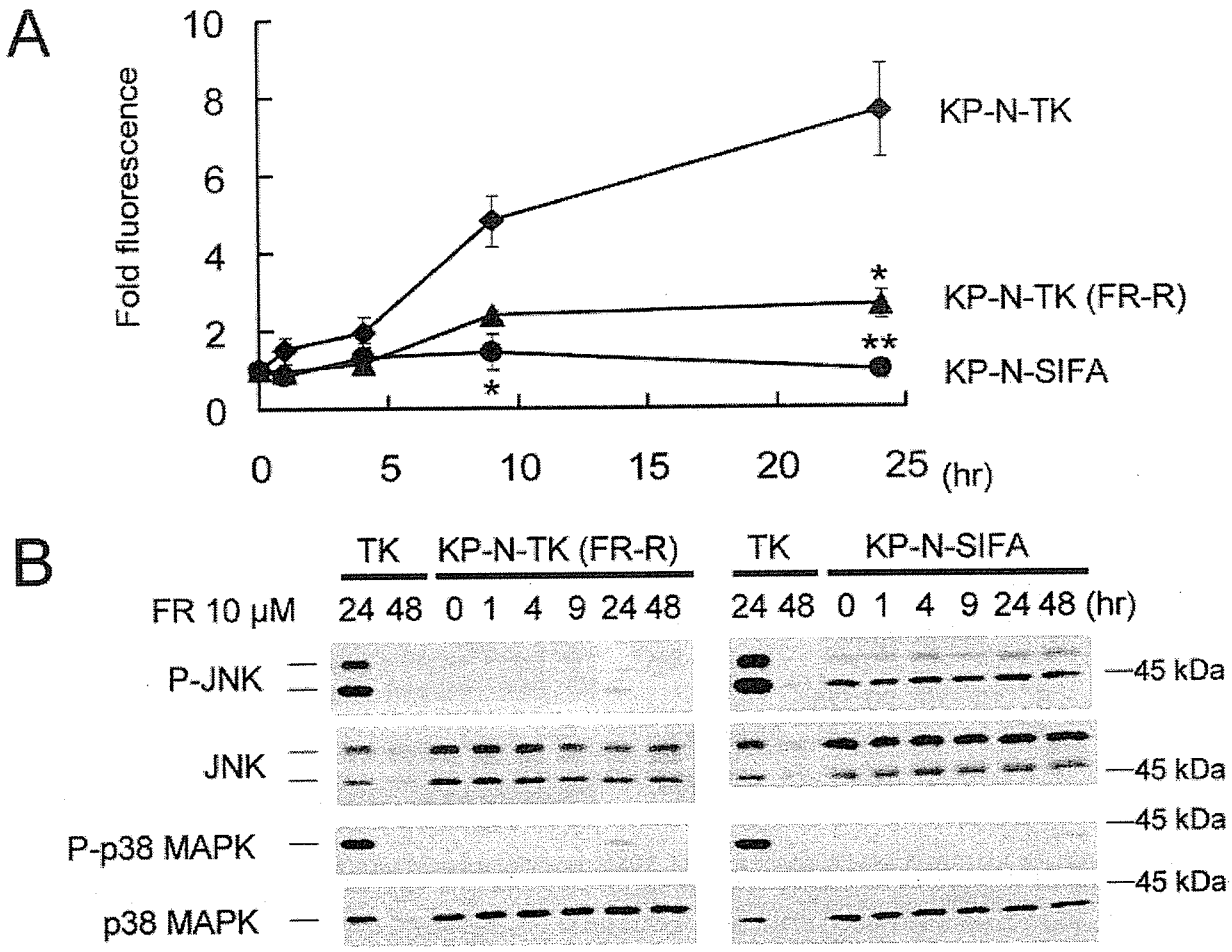

FIGURE 3 – Fenretinide-induced ROS accumulation and activation of JNK and p38 MAPK is suppressed in FR-resistant KP-N-TK (FR-R) and KP-N-SIFA cells. (*a*) Time-course of intracellular ROS. Cells were incubated with 10 μM FR for the times indicated. CM-H_2DCFDA was added for 2 hr before cell harvesting. Flow cytometric analysis was carried out and the mean fluorescence was calculated (mean ± SD, $n = 3$). $*p < 0.05$, $**p < 0.01$ (compared to KP-N-TK, Student's *t*-test). (*b*) Time-course of activation of JNK and p38 MAPK. Cells were treated with 10 μM FR for the times indicated. Immunoblotting was carried out as described above. This is representative of 3 independent experiments.

Furthermore, preincubation of AA suppressed FR-induced intracellular ROS accumulation in KP-N-TK cells (Fig. 2*c*). To determine whether FR-induced activation of JNK and p38 MAPK is ROS-dependent, we compared the phosphorylation of JNK and p38 MAPK induced by FR with or without preincubation with AA in KP-N-TK cells. In the presence of AA, FR-induced activation of JNK and p38 MAPK was suppressed markedly (Fig. 2*d*).

Fenretinide-induced intracellular ROS accumulation and activation of JNK and p38 MAPK is decreased in fenretinide-resistant NB cell lines

To investigate the mechanism of resistance to FR in NB cells, we generated a FR-resistant KP-N-TK cell line, KP-N-TK (FR-R) cells. KP-N-TK (FR-R) was highly resistant to FR even at a concentration of 10 μM FR (data not shown). When KP-N-TK (FR-R) was incubated in FR-free medium, its resistance to FR was preserved (data not shown). KP-N-SIFA cells exhibited complete resistance to 10 μM FR (data not shown).

To determine whether FR-induced intracellular ROS production was altered in the resistant NB cells, we treated FR-resistant KP-N-TK (FR-R) cells, KP-N-SIFA cells and FR-sensitive parental KP-N-TK cells with 10 μM FR and compared their intracellular ROS levels. Less FR-induced intracellular ROS were generated in the 2 resistant cell lines than in the sensitive KP-N-TK cells (Fig. 3*a*).

FR induced little phosphorylation of the kinases in the resistant KP-N-TK (FR-R) and KP-N-SIFA cells (Fig. 3*b*). Although phosphorylated JNK was present in KP-N-SIFA cells even in the absence of FR, FR did not increase its level during 48 hr.

DISCUSSION

FR is known to induce apoptosis in NB cells but the mechanism is not clear. Our results demonstrate that FR induced sustained-activation of JNK and p38 MAPK signaling in an ROS-dependent manner, and finally induced apoptosis in NB cells. In FR-resistant NB cells, FR failed not only to generate intracellular ROS but also to activate JNK and p38 MAPK signaling. Thus, the alterations in FR-resistant NB cells prevent FR from inducing apoptosis.

ROS are known to induce apoptosis. In KP-N-TK cells, FR induces prolonged production of intracellular ROS. FR-induced ROS generation precedes the processing of caspase-9, caspase-3 and PARP, indicating that ROS generation is upstream of the

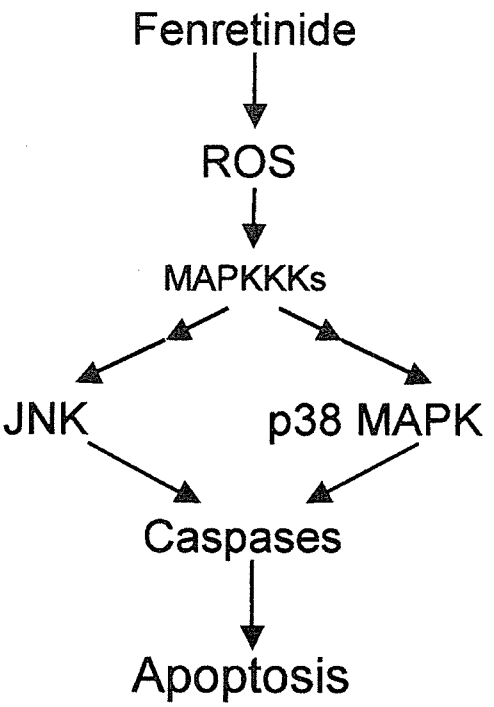

FIGURE 4 – Schematic representation of FR-induced ROS generation, JNK and p38 MAPK signaling and apoptosis in neuroblastoma cells. FR induces sustained-activation of JNK and p38 MAPK signaling in an ROS-dependent manner. The sustained activation of JNK and p38 MAPK activation leads to processing of caspases and apoptosis.

caspase cascade. The antioxidant AA almost completely blocked apoptosis and suppressed FR-induced intracellular ROS accumulation. Our results show that AA has a more complete inhibitory effect on FR-induced apoptosis in NB cells than on FR-induced apoptosis in other NB cell lines (CHLA-90, SMS-LHN, SMS-KCNR[7] and SH-SY5Y[8]).

FR activated both JNK and p38 MAPK in FR-sensitive KP-N-TK NB cells. In KP-N-TK cells, the activation of JNK and p38 MAPK by FR (starting after 4 hr of FR treatment) preceded the cleavages of caspase-9, caspase-3 and PARP (starting after 24 hr of FR treatment), indicating that the JNK and p38 MAPK signaling pathways are upstream of the caspase cascades, as reported in the LNCap and PC3 prostate carcinoma cell lines.[16,17] Furthermore, FR-induced activation of JNK and p38 MAPK is sustained for 48 hr, suggesting the possible role of the signaling in FR-induced apoptosis.[13–15] Interestingly, in prostate carcinoma LNCap cells, FR activated JNK but not p38 MAPK.[16]

Our finding that FR-induced activation of JNK and p38 MAPK in NB cells was ROS-dependent is supported by the finding that AA suppressed FR-induced activation of JNK and p38 MAPK signaling in KP-N-TK cells. In prostate carcinoma cells, Chen *et al.*[16] found that FR-induced JNK activation was not affected by the antioxidant *N*-acetyl-L-cysteine (NAC), indicating that FR activated JNK independent of ROS. They did not, however, determine whether NAC suppressed the accumulation of FR-induced intracellular ROS. In our present study, AA clearly reduced FR-induced intracellular ROS accumulation.

JNK and p38 MAPK pathways have been shown to be involved in ROS-induced apoptosis.[13,14] When ROS production is low, JNK and p38 MAPK are only transiently activated, and cells will survive.[13,14] On the contrary, high ROS production induces sustained-activation of JNK and p38 MAPK, and finally leads to cell death.[13,14] The quantity and duration of oxidative stress will determine which MAPK kinase kinases (MAPKKK) are activated, which will determine the activation pattern of JNK and p38 MAPK, which, in turn, will decide cell fate.[13,14]

ROS activate various signaling pathways other than MAPKKK, including c-Abl tyrosine kinase.[14] c-Abl activates both JNK and p38 MAPK in the response to DNA damage[22] and also mediates ROS-induced apoptosis under some conditions.[23] The c-Abl-p38 MAPK-p73 pathway is thought to be essential for apoptosis induced by chemotherapeutic agents.[24] This pathway might be also involved in fenretinide-induced apoptosis, although we did not examine the expression of p73 in these cells.

FR failed to induce intracellular ROS accumulation in the FR-resistant KP-N-TK (FR-R) and KP-N-SIFA NB cell lines, indicating that suppression of the ROS-productive system is responsible for the resistance to FR in NB cells. Similarly, FR produced less free radicals in FR-resistant SH-SY5Y cells.[8] ROS production in the FR-resistant A2780 ovarian cancer cell line was not significantly different from that in the FR-sensitive parental cells.[21] In FR-resistant NB cells, FR failed to activate JNK and p38 MAPK signaling. This result further supports the hypothesis that FR activates JNK and p38 MAPK signaling in an ROS-dependent manner. It also indicates that sustained-activation of JNK and p38 MAPK is responsible for FR-induced apoptosis. It is of interest to know whether these FR-resistant cells are also resistant to other cytotoxic agents, especially ROS-producing ones such as cisplatin. In our preliminary results, FR-resistant KP-N-SIFA cells were the most sensitive to cisplatin among the cell lines used in our study (data not shown). KP-N-TK cells, as well as KP-N-TK (FR-R) cells, were resistant to 20 μM cisplatin (data not shown). These data suggest that the mechanisms of FR resistance and cisplatin resistance are different.

In conclusion, we demonstrated for the first time that FR induces sustained activation of JNK and p38 MAPK in an ROS-dependent manner in FR-sensitive NB cells (Fig. 4), but not in FR-resistant cells. Moreover, our results raise the possibility that sustained-activation of the stress signaling pathway mediates FR-induced apoptosis. Our results also show for the first time that suppression of the intracellular ROS productive system and the downstream JNK/p38 MAPK pathways are related to FR-resistance in NB cells.

ACKNOWLEDGEMENTS

We gratefully acknowledge Dr. H. Ichijo (Laboratory of Cell Signaling, Graduate School of Pharmaceutical Sciences, The University of Tokyo) and all the members of our laboratory for their valuable discussions and support.

REFERENCES

1. Matthay KK, Castleberry RP. Treatment of advanced neuroblastoma. The US experience. In: Brodeur GM, Sawada T, Tsuchida Y, Voute PA, eds. Neuroblastoma. Amsterdam: Elsevier Science Publishers B.V., 2000. 417–36.
2. Sugimoto T, Sawada T, Matsumura T, Horii Y, Kemshead JT, Suzuki Y, Okada M, Tagaya O, Hino T. Morphological differentiation of human neuroblastoma cell lines by a new synthetic polyprenoic acid (E5166). Cancer Res 1987;47:5433–8.
3. Matthay KK, Villablanca JG, Seeger RC, Stram DO, Harris RE, Ramsay NK, Swift P, Shimada H, Black CT, Brodeur GM, Gerbing RB, Reynolds CP. Treatment of high-risk neuroblastoma with intensive chemotherapy, radiotherapy, autologous bone marrow transplantation, and 13-cis retinoic acid. N Engl J Med 1999;341:1165–73.
4. Wu JM, DiPietrantonio AM, Hsieh T-C. Mechanism of fenretinide (4-HPR)-induced cell death. Apoptosis 2001;6:377–88.
5. Rotmensz N, De Palo G, Formelli F, Costa A, Marubini E, Campa T, Crippa A, Danesini GM, Delle Grottaglie M, Di Mauro MG, Filiberti A, Gallazzi M, et al. Long-term tolerability of fenretinide (4-HPR) in breast cancer patients. Eur J Cancer 1991;27:1127–31.
6. Garaventa A, Luksch R, Lo Piccolo MS, Cavadini E, Montaldo PG,

Pizzitola MR, Boni L, Ponzoni M, Decensi A, De Bernardi B, Bellani FF, Formelli F. Phase I trial and pharmacokinetics of fenretinide in children with neuroblastoma. Clin Cancer Res 2003;9:2032–9.
7. Maurer BJ, Metelitsa LS, Seeger RC, Cabot MC, Reynolds CP. Increase of ceramide and induction of mixed apoptosis/necrosis by N-(4-hydroxyphenyl)-retinamide in neuroblastoma cell lines. J Natl Cancer Inst 1999;91:1138–46.
8. Lovat PE, Ranalli M, Annichiarrico-Petruzzelli M, Bernassola F, Piacentini M, Malcolm AJ, Pearson ADJ, Melino G, Redfern CPF. Effector mechanisms of fenretinide-induced apoptosis in neuroblastoma. Exp Cell Res 2000;260:50–60.
9. Lovat PE, Oliverio S, Ranalli M, Corazzari M, Rodolfo C, Bernassola F, Aughton K, Maccarrone M, Campbell Hewson QD, Pearson ADJ, Melino G, Piacentini M, et al. GADD153 and 12-lipoxygenase mediate fenretinide-induced apoptosis of neuroblastoma. Cancer Res 2002;62:5158–67.
10. Maurer BJ, Melton L, Billups C, Cabot MC, Reynolds CP. Synergistic cytotoxicity in solid tumor cell lines between N-(4-hydroxyphenyl)-retinamide and modulators of ceramide metabolism. J Natl Cancer Inst 2000;92:1897–909.
11. Wang H, Maurer BJ, Reynolds CP, Cabot MC. N-(4-hydroxyphenyl)-retinamide elevates ceramide in neuroblastoma cell lines by coordinate activation of serine palmitoyltransferase and ceramide synthase. Cancer Res 2001;61:5102–5.
12. Kyriakis JM, Avruch J. Mammalian mitogen-activated protein kinase signal transduction pathways activated by stress and inflammation. Physiol Rev 2001;81:807–69.
13. Matsuzawa A, Nishitoh H, Tobiume K, Takeda K, Ichijo H. Physiological roles of ASK1-mediated signal transduction in oxidative stress- and endoplasmic reticulum stress-induced apoptosis: advanced findings from ASK1 knockout mice. Antioxid Redox Signal 2002;4:415–25.
14. Martindale JL, Holbrook NJ. Cellular response to oxidative stress: signaling for suicide and survival. J Cell Physiol 2002;192:1–15.
15. Xia Z, Dickens M, Raingeaud J, Davis RJ, Greenberg ME. Opposing effects of ERK and JNK-p38 MAP kinases on apoptosis. Science 1995;270:1326–31.
16. Chen Y-R, Zhou G, Tan T-H. c-Jun N-terminal kinase mediates apoptotic signaling induced by N-(4-hydroxyphenyl)retinamide. Mol Pharmacol 1999;56:1271–9.
17. Shimada K, Nakamura M, Ishida E, Kishi M, Yonehara S, Konishi N. Contributions of mitogen-activated protein kinase and nuclear factor kappa B to N-(4-hydroxyphenyl)- retinamide-induced apoptosis in prostate cancer cells. Mol Carcinogen 2002;35:127–37.
18. Ulukaya E, Pirianov G, Kurt MA, Wood EJ, Mehmet H. Fenretinide induces cytochrome c release, caspase 9 activation and apoptosis in the absence of mitochondrial membrane depolarization. Cell Death Differ 2003;10:856–9.
19. Kuroda H, Sugimoto T, Horii Y, Sawada T. Signaling pathway of ciliary neurotrophic factor in neuroblastoma cell lines. Med Pediatr Oncol 2001;36:118–21.
20. Sugimoto T, Horii Y, Hino T, Kemshead JT, Kuroda H, Sawada T, Morioka H, Imanishi J, Inoko H. Differential susceptibility of HLA class II antigens induced by γ-interferon in human neuroblastoma cell lines. Cancer Res 1989;49:1824–8.
21. Appierto V, Cavadini E, Pergolizzi R, Cleris L, Lotan R, Canevari S, Formelli F. Decrease in drug accumulation and in tumour aggressiveness marker expression in a fenretinide-induced resistant ovarian tumour cell line. Br J Cancer 2001;84:1528–34.
22. Kharbanda S, Yuan Z-M, Weichselbaum R, Kufe D. Determination of cell fate by c-Abl activation in the response to DNA damage. Oncogene 1998;17:3309–18.
23. Sun X, Majumder P, Shioya H, Wu F, Kumar S, Weichselbaum R, Kharbanda S, Kufe D. Activation of the cytoplasmic c-Abl tyrosine kinase by reactive oxygen species. J Biol Chem 2000;275:17237–40.
24. Melino G, De Laurenzi V, Vousden KH. p73: Friend or foe in tumorigenesis. Nat Rev Cancer 2002;2:605–15.

Int. J. Cancer: **112**, 365–375 (2004)

Publication of the International Union Against Cancer

LOW EXPRESSION OF HUMAN TUBULIN TYROSINE LIGASE AND SUPPRESSED TUBULIN TYROSINATION/DETYROSINATION CYCLE ARE ASSOCIATED WITH IMPAIRED NEURONAL DIFFERENTIATION IN NEUROBLASTOMAS WITH POOR PROGNOSIS

Chiaki KATO[1,2], Kou MIYAZAKI[1], Atsuko NAKAGAWA[3], Miki OHIRA[1], Yohko NAKAMURA[1], Toshinori OZAKI[1], Toshio IMAI[2] and Akira NAKAGAWARA[1]*

[1]*Division of Biochemistry, Chiba Cancer Center Research Institute, Chiba, Japan*
[2]*Department of Physiologic Chemistry Faculty of Science, Toho University, Chiba, Japan*
[3]*Second Department of Pathology, Aichi Medical University, Nagakute, Japan*

Neuroblastoma (NBL), one of the most common childhood solid tumors, has a distinct nature in different prognostic subgroups. However, the precise mechanism underlying this phenomenon remains largely unknown. To understand the molecular and genetic bases of neuroblastoma, we have generated its cDNA libraries and identified a human ortholog of *tubulin tyrosine ligase* gene (*hTTL*/*Nbla0660*) as a differentially expressed gene at high levels in a favorable subset of the tumor. Tubulin is subjected to several types of evolutionarily conserved posttranslational modification, including tyrosination and detyrosination. Tubulin tyrosine ligase catalyzes ligation of the tyrosine residue to the COOH terminus of the detyrosinated form of α-tubulin. The measurement of *hTTL* mRNA expression in 74 primary neuroblastomas by quantitative real-time reverse transcription-PCR revealed that its high expression was significantly associated with favorable stages (1, 2 and 4s; $p = 0.0069$), high *TrkA* expression ($p = 0.002$), a single copy of *MYCN* ($p < 0.00005$), tumors found by mass screening ($p = 0.0042$), nonadrenal origin ($p = 0.0042$) and good prognosis ($p = 0.023$). The log-rank test showed that high expression of *hTTL* was an indicator of favorable prognosis ($p = 0.026$). Immunohistochemical analysis using specific antibodies generated by us demonstrated that tyrosinated tubulin (Tyr-tubulin), detyrosinated tubulin (Glu-tubulin) and hTTL as well as Δ2-tubulin were positive in favorable tumors, whereas only Δ2-tubulin was positive in the tumors with *MYCN* amplification. In an RTBM1 neuroblastoma cell line, hTTL was increased after treating the cells with bone morphogenetic protein 2 (BMP2) or all-trans retinoic acid (RA), which induced neuronal differentiation. These results suggest that the deregulated tubulin tyrosination/detyrosination cycle caused by decreased expression of hTTL is associated with inhibition of neuronal differentiation and enhancement of cell growth in the primary neuroblastomas with poor outcome.

Key words: *tubulin tyrosine ligase; tubulin tyrosination; neuroblastoma; neuronal differentiation; prognostic factor*

Tubulin is one of the most important molecular components that regulate cytoskeletal structure relating to cell motility, cell division, differentiation, invasion and metastasis in cancer. However, functional modification of tubulin protein has still been elusive. Tubulin is subjected to several types of evolutionarily conserved posttranslational modification that includes tyrosination/detyrosination, acetylation, phosophorylation, palmitoylation, polyglutamylation and polyglycylation.[1–4] The discovery of tyrosination cycle stems from the serial observations that the addition of radiolabeled tyrosine to a rat brain cytosolic extract leads to tyrosination of the COOH terminus of a single endogenous protein, α-tubulin, by a translation-independent mechanism.[5–7] Posttranslational incorporation of tyrosine into the tubulin has also been shown to occur *in vivo*.[8–10] The cycle of tyrosination/detyrosination is evolutionarily conserved[11–13] and is regulated by both tubulin tyrosine ligase (TTL) and carboxypeptidase, the gene of which has not yet been identified (Fig. 1). Microtubule dynamics is also an important factor. TTL protein was first purified by immunoaffinity chromatography from the lysates of bovine and porcine brains and was extensively characterized by protein sequencing.[14] Recently, rat *TTL* cDNA has also been isolated.[15] Interestingly, in 1991, Paturle-Lafanechere *et al.*[16] identified a nontyrosinatable variant of tubulin that lacked 2 amino acid residues, glutamic acid and tyrosine, at the COOH terminus (Δ2-tubulin). Δ2-tubulin was found to accumulate in mature neurons and in stable microtubule assemblies in cells.[17,18] In some tumors, it also accumulated in the cellular cytoplasm in association with decreased levels of TTL, suggesting that the amount of Δ2-tubulin and TTL expression level in tumor cells are important to define the malignant grade of cancer.[19] However, pathophysiologic significance of the tyrosination/detyrosination cycle in normal and cancer cells still remains unclear.

Neuroblastoma (NBL) is one of the most common childhood solid tumors and has distinct biologic characteristics in different prognostic subgroups. For example, NBL in patients under 1 year of age usually regresses spontaneously, whereas that in patients over 1 year of age often grows aggressively and eventually kills the patient. To understand the molecular mechanism of distinct biology and tumorigenesis of NBL, we have previously performed a comprehensive approach to unveil the gene expression profiles among the NBL subsets.[20,21] We constructed the subset-specific oligo-capping cDNA libraries from the primary NBL tissues with favorable (stage 1, high expression of *TrkA* and a single copy of *MYCN*) and unfavorable (stage 3 or 4, decreased expression of *TrkA* and *MYCN* amplification) characteristics and randomly cloned 4,654 cDNAs. After adding the cDNAs obtained from the stage 4s NBL cDNA library to our NBL gene collection, we made an in-house cDNA microarray carrying 5,340 genes proper to NBL. The comprehensive analysis of 136 NBLs using the microar-

Abbreviations: BMP2, bone morphogenetic protein 2; DMEM, Dulbecco's modified Eagle's medium; ECL, enhanced chemiluminescence; FBS, fetal bovine serum; hTTL, human tubulin tyrosine ligase; NBL, neuroblastoma; RA, retinoic acid; TCP, tubulin carboxypeptidase; TTL, tubulin tyrosine ligase.

Grant sponsor: Grant-in-Aid for Scientific Research and for Scientific Research on Priority Areas, Medical Genome Science from the Ministry of Education, Science, Sports and Culture, Japan; Grant sponsor: Hisamitsu Pharmaceutical Co. Inc.

*Correspondence to: Division of Biochemistry, Chiba Cancer Center Research Institute, 666-2 Nitona, Chuoh-ku, Chiba 260-8717, Japan. Fax: +81-43-265-4459. E-mail: akiranak@chiba-ccri.chuo.chiba.jp

Received 27 January 2004; Accepted 15 April 2004

DOI 10.1002/ijc.20431
Published online 23 June 2004 in Wiley InterScience (www.interscience.wiley.com).

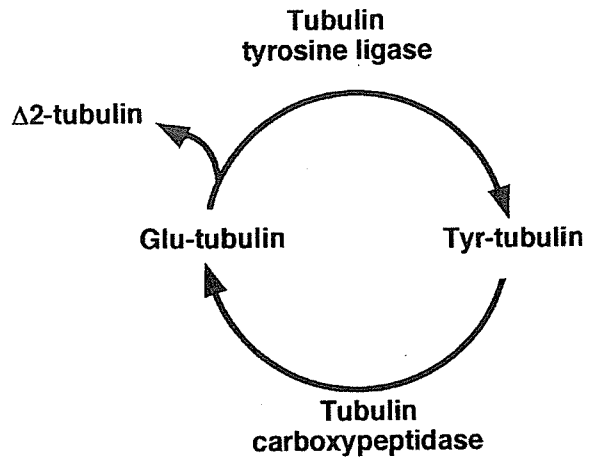

FIGURE 1 – The tyrosination/detyrosination cycle catalyzed by tubulin tyrosine ligase and tubulin carboxypeptidase.

ray showed that many genes that are related to the cytoskeletal components, including α-tubulin, had prognostic significance (data not shown).

In the present study, we have cloned for the first time the human ortholog of TTL (*hTTL*) from both the NBL and a fetal brain cDNA libraries. The analysis using 74 primary NBLs shows that expression of *hTTL* mRNA is significantly lower in unfavorable NBLs than in favorable tumors. The examination using specific antibodies raised against hTTL, Tyr-tubulin, Glu-tubulin and Δ2-tubulin demonstrates that hTTL is increased during induction of neuronal differentiation of cultured NBL cells treated with BMP2 or RA. The immunohistochemical study shows that hTTL, Tyr-tubulin, Glu-tubulin and Δ2-tubulin are positive in favorable NBLs, whereas only Δ2-tubulin is positive in aggressive NBLs with *MYCN* amplification. These suggested that the tyrosination/detyrosination cycle of α-tubulin is active in NBLs with high potential to differentiate or undergo apoptosis, while it is disregulated by downregulation of hTTL in *MYCN*-amplified NBLs, resulting in accumulation of Δ2-tubulin.

MATERIAL AND METHODS

Tumor specimen

Fresh frozen tumor tissues obtained by surgery or biopsy were sent to the Division of Biochemistry, Chiba Cancer Center Research Institute, from various hospitals in Japan with informed consent. Ninety tumors examined in this study were staged according to the International Neuroblastoma Staging System (INSS).[22] The number of tumors subjected to quantitative real-time RT-PCR were 24 in stage 1, 11 in stage 2, 5 in stage 4s, 10 in stage 3 and 24 in stage 4. The patients were treated according to the protocols previously described.[23] Biologic information on each tumor, including *MYCN* gene copy number, *TrkA* gene expression and DNA ploidy, was analyzed in our laboratory as described previously.[24]

Cell culture and transfection

COS7 and HEK293T cells were maintained in Dulbecco's modified Eagle's medium (DMEM) supplemented with 10% heat-inactivated fetal bovine serum (FBS; Life Technologies, Gaithersburg, MD) and penicillin (100 IU/ml)/streptomycin (100 μg/ml). Human neuroblastoma RTBM1 cells were grown in RPMI-1640 medium containing 10% heat-inactivated FBS and antibiotic mixture. Cultures were maintained at 37°C in a water-saturated atmosphere of 5% CO_2 in air. Transient transfection was performed by LipofectAMINE 2000 transfection reagent (Invitrogen, Carlsbad, CA) according to the manufacturer's instructions. In brief, cells were seeded in tissue culture plates to achieve 50% confluence. Twenty-four hours later, cells were transfected by using a mixture of the expression plasmids and LipofectAMINE 2000 transfection reagent in DMEM without serum. Forty-eight hours after transfection, cells were collected and analyzed by Western blotting. For neurite extension assays, RTBM1 cells were treated either with recombinant human BMP2 (Yamanouchi Pharmaceutical, Tokyo, Japan) or with RA at a final concentration of 1 nM or 5 μM, respectively.

RNA isolation and semiquantitative RT-PCR

Total RNA was prepared from neuroblastoma tissues according to the AGPC method.[25] Five micrograms of total RNA were subjected to the synthesis of the first-strand cDNA with pd$(N)_6$ random hexamer (Takara Shuzo, Otsu, Japan) and a Superscript II reverse transcriptase (Invitrogen) at 42°C for 90 min. The resultant cDNA was diluted to be a 1:20 solution and was amplified in a final volume of 10 μl of reaction mixture containing 100 μM of each deoxynucleoside triphosphate, 1 × PCR buffer, 1 μM of each primer and 0.2 U of rTaq DNA polymerase (Takara Bio, Ohtsu, Japan). The following primers were used: *hTTL*, 5′-CAGCTCTTCGGCTTTGACTT-3′ (sense) and 5′-GCTGTGGGCTGGATAAAGAG-3′ (antisense); human *GAPDH*, 5′-ACCTGACCTGCCGTCTAGAA-3′ (sense) and 5′-TCC ACCACCCTGTTGCTGTA-3′ (antisense). PCR templates were standardized by its *GAPDH* expression before performing semiquantitative PCR experiment. The PCR-amplified products were separated by electrophoresis on a 1.5% agarose gel and visualized by ethidium bromide poststaining.

Quantitative real-time RT-PCR

cDNA was prepared by the same method as in the semiquantitative RT-PCR and 2 μl of the 40-fold dilution was used for each PCR reaction. Primers and TaqMan probes for *hTTL* were designed using the primer design software Primer Express (Perkin-Elmer Applied Biosystems, Foster City, CA). The primer sequences for *hTTL* are 5′-AAGGAACTGCCTCCTGAGC-3′ and 5′-TCAATGAGCCAC ACCTTCA-3′. The probe sequence for *TTL* is 5′-FAM-ATTAGC ACCAAGCACCTCCCTTACCAGAGC-TAMRA-3′. PCR was carried out with the ABI Prism 7700 Sequence Detection System (Perkin-Elmer Applied Biosystems). Two μl of cDNA was amplified in a final volume of 25 μl containing 1 × TaqMan mixture, 300 nM each primer and 200 nM TaqMan probe. The thermal cycling condition was as follows: 50 cycles of a 2-step PCR (95°C for 15 sec, 60°C for 1 min) after the initial activation of UNG followed by denaturation (50°C for 2 min, 95°C for 10 min). TaqMan *GAPDH* control reagent kit (Roche Molecular Biochemicals, Basel, Switzerland) was used for the amplification of *GAPDH* according to the manufacturer's instructions; all data were normalized using *GAPDH* expression. The experiments were performed in triplicate for each data point.

Generation of polyclonal anti-hTTL antibodies

The polyclonal anti-hTTL antibody was raised in rabbits against Cys-coupled synthetic peptides derived from hTTL (222-RTASEPY-HVDNFQDKTCHLTNH-243 and 244-CIQKEYSKNYGKYEE-GNE-261). The polyclonal anti-Tyr-tubulin, anti-Glu-tubulin and anti-Δ2-tubulin antibodies were raised in rabbits immunized with Cys-coupled synthetic peptides corresponding to their COOH termini (CEEEGEEY, CGEEEGEE and CEGEEEGE, respectively). Antibodies were purified by using peptide-coupled affinity columns and tested for their ability to identify the corresponding proteins by Western blots. The synthetic peptides and antibodies were generated by Protein Express (Chiba, Japan).

Construction of FLAG-tagged hTTL expression plasmid

The FLAG-tagged hTTL expression plasmid was generated by PCR amplification using the cDNA library derived from human fetal brain (Stratagene, La Jolla, CA) and an *hTTL* cDNA that lacked the 5′-portion encoding the NH_2 terminal region of hTTL as templates. The forward and reverse primers used were 5′-TAAATAGTCGACGATATC**ATGGACTACAAGGACGAC**

GACGACAAGTACACCTTCGTGGTACGCGATGAGAACAGC AGCGTCTACGCCGAGGTCTCCCGGCTGCTCCTCGCCA-3′ (sequence encoding FLAG epitope tag is in boldface, and *Eco*RV recognition site is underlined) and 5′-TACATGTCGACGCGG CCGCTCACAGCTTGAT GAA-3′ (*Not*I restriction site is underlined). The resulting PCR product was gel-purified, digested with *Eco*RV and *Not*I, inserted into identical restriction sites of a mammalian expression plasmid pIRESpuro2 (Clontech Laboratories, Palo Alto, CA) and its nucleotide sequence was verified by automated dideoxy terminator cycle sequencing.

Western blot analysis

Cells were washed in ice-cold phosphate-buffered saline (PBS), collected by centrifugation and lysed in 1 × sample buffer. Equal amounts of whole-cell lysates were fractionated by SDS-polyacrylamide gel electrophoresis (SDS-PAGE), and electrophoretically transferred onto a polyvinylidene difluoride (PVDF) membrane filter (Immobilon-P; Millipore, Billerica, MA). The filter was then blocked with Tris-buffered saline (TBS) containing 5% nonfat dry milk at room temperature for 1 hr and subsequently incubated for 1 hr with the antibodies against hTTL, Tyr-tubulin, Glu-tubulin, Δ2-tubulin, α-tubulin (5H1; PharMingen, San Diego, CA) and actin (20-33; Sigma Chemical, St. Louis, MO). The filter was further incubated with horseradish peroxidase-conjugated mouse or rabbit IgG secondary antibody (Cell Signaling Technologies, Beverly, MA). Immunoreactivity was detected using the enhanced chemiluminescence system (ECL; Amersham Pharmacia Biotechnology, Uppsala, Sweden) according to the manufacturer's instructions. The films were exposed at multiple time points to ensure that the images were not saturated.

Immunohistochemistry

Immunohistochemical stainings with antibodies against hTTL (1:100), Tyr-tubulin (1:100), Glu-tubulin (1:100) and Δ2-tubulin (1:100) were performed on 10 human neuroblastoma tumors selected from the surgical pathology file at the Department of Pathology, Aichi Medical University, based on the results of histopathology evaluation[26] and *MYCN* status. Also performed were immunostainings with antibodies against TrkA (1:40, 763; Santa Cruz Biotechnology, Santa Cruz, CA), CD56 (1B6; Novocastra Laboratories, Peterborough, U.K.) and Ki-67 (1:200, MIB-1; Dako, Kyoto, Japan) on the same tumor tissues. All of those tumor samples were obtained prior to chemotherapy and irradiation therapy and included 6 favorable histology cases with nonamplified *MYCN* (FH&NA) and 4 unfavorable histology cases with amplified *MYCN* (UH&A). Among the neuroblastoma cases, tumors in the FH&NA subset were reported to be the most favorable biologically and clinically. In contrast, tumors in the UH&A subset are known to be the most aggressive with the poorest clinical outcome.[27] Four μm thick sections from the formalin-fixed and paraffin-embedded tissue samples were deparaffinized and microwaved for 3 × 5 min in Na-citrate buffer (pH 6.0) for antigen retrieval. The slides were first immersed in 0.3% hydrogen peroxide in methanol for 20 min and then in 10% normal goat serum for 30 min. The primary antibodies were then applied at 4°C overnight, followed by a standard staining procedure using the Vectastain ABC kit (Vector Laboratories, Burlingame, CA). Sections were counterstained with hematoxylin for light microscopic review and evaluation. hTTL, Tyr-tubulin, Glu-tubulin and Δ2-tubulin were always positively detected in the cytoplasm and neuritic processes of normal ganglion cells in the separate positive control sections as well as in the test sections as built-in control, whenever available. As for the negative controls of hTTL, Tyr-tubulin, Glu-tubulin, Δ2-tubulin and TrkA stainings, normal rabbit immunoglobulins (1:500 dilution, Vector Laboratories) were applied as the primary antibody. As for the negative controls of CD56 and Ki-67 stainings, we followed the staining procedure without the primary antibodies.

Statistical analysis

Student's *t*-tests were used to explore possible associations between *hTTL* expression and other factors, such as age. Since the values of the *hTTL* expression were skewed, a log transformation was used to achieve the normality when using *t*-test and Cox regression. The distinction between high and low levels of *hTTL* was based on the median value (low, *hTTL* < 95 e.u.; high, *hTTL* > 95 e.u.), regardless of tumor stage, *MYCN* copy number, or survival. Kaplan-Meier survival curves were calculated, and survival distributions were compared using the log-rank test. Cox regression models were used to explore associations between *hTTL* expression, age, *MYCN* amplification, mass screening, origin and survival. Statistical significance was declared if the *p*-value was < 0.05. Statistical analysis was performed using Stata 7.0. (Stata, College Station, TX).

RESULTS

Cloning and expression of hTTL *gene*

We have previously constructed oligo-capping cDNA libraries from 3 fresh human NBL tissues (stages 1 and 2, high *TrkA* expression and a single copy of *MYCN*), which were gradually undergoing spontaneous regression probably due to neuronal apoptosis.[20] Screening of 1,152 novel genes by reverse transcriptase (RT)-PCR revealed that 194 genes were expressed differentially between NBLs with favorable prognosis and those with unfavorable outcome. Among them, we detected a partial cDNA sequence (*Nbla00660*) corresponding to the human ortholog of *tubulin tyrosine ligase* (*hTTL*) gene. We then cloned the full-length *hTTL* cDNA using both conventional phage library screening and genome sequence-based RT-PCR procedure. The *hTTL* gene was mapped to chromosome 2q13 and consisted of 7 exons (Fig. 2*a*) with 377 predicted amino acids (Genbank/DDBJ accession number AB071393; Fig. 2*b*). Comparison of the deduced amino acid sequence of human *TTL* cDNA with those of mouse, rat, pig and cow showed identity by 94%, 94%, 93% and 94%, respectively. *hTTL* was ubiquitously expressed in various human tissues including heart, kidney, lung, colon, thymus, spleen, mammary gland, testis, prostate, brain, cerebellum, liver, fetal brain, fetal liver, adrenal gland and skeletal muscle (Fig. 2*c*). However, it was rather preferentially expressed in adult and fetal brains and lung.

Specific antibodies and catalytic activity of hTTL

To study the role of hTTL and the tyrosination/detyrosination cycle regulated by TTL in neuroblastoma, we generated specific antibodies against human Tyr-tubulin, Glu-tubulin and Δ2-tubulin based on the previous reports.[16,18,28] The PVDF membranes spotted with equal amount (1 μg) of synthetic peptides corresponding to COOH terminal 7 amino acid residues of Tyr-tubulin (CEEEGEEY), Glu-tubulin (CGEEEGEE) and Δ2-tubulin (CEGEEEGE) were immunoblotted with rabbit anti-Tyr-tubulin antibody (Fig. 3*a*, top), anti-Glu-tubulin antibody (Fig. 3*a*, middle) and anti-Δ2-tubulin antibody (Fig. 3*a*, bottom), respectively. There were no crossreactivities among them, suggesting that those 3 antibodies were highly specific to each form of tubulin. To confirm the catalytic activity of hTTL encoded by the gene we cloned, we transfected the HEK293T cells with various amount of *hTTL* expression construct. Increased levels of hTTL in those cells induced tyrosination of tubulin in dose-dependent manner, while the level of endogenous Glu-tubulin was decreased (Fig. 3*c*). These results showed that hTTL protein encoded by the gene we cloned has its catalytic activity.

Upregulation of hTTL expression during neuronal differentiation

BMP2 has been characterized as a neurotrophic factor.[29] Recently, Nakamura *et al.*[30] have reported that RTBM1, a human neuroblastoma cell line, is responsive to both BMP2 and RA by extending neurites. By using this system, we examined whether the expression levels of hTTL change during induction of neuronal differentiation. As shown in Figure 4, the treatment of RTBM1

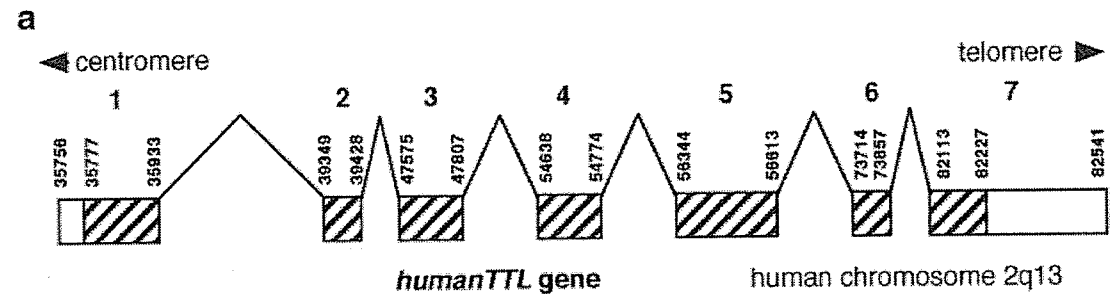

b

```
humanTTL  MYTFVVRDENSSVYAEVSRLLLATGHWKRLRRDNPRFNLMLGERNRLPFGRLGHEPGLVQLVNYYRGADKLCRKAS 76
mouseTTL  MYTFVVRDENSSVYAEVSRLLLATGYWKRLRRDNPRFNLMLGERNRLPFGRLGHEPGLAQLVNYYRGADKLCRKAS 76
ratTTL    MYTFVVRQENSSVYAEVSRLLLATGYWKRLRRDNPRFNLMLGGRNRLPFGRLGHEPGLAQLVNYYRGADKLCRKAS 76
pigTTL    MYTFVVRDENSSVYAEVSRLLLATGHWKRLRRDNPRFNLMLGERNRLPFGRLGHEPGLMQLVNYYRGADKLCRKAS 76
cowTTL    MYTFVVRDENSSVYAEVSRLLLATGHWKRLRRDNPRFNLMLGERNRLPFGRLGHEPGLMQLVNYYRGADKLCRKAS 76
          ******* ***************** ***************** ***************** ****************

humanTTL  LVKLIKTSPELAESCTWFPESYVIYPTNLKTPVAPAQNGIQPPISNSRTDEREFFLASYNRKKEDGEGNVWIAKSS 152
mouseTTL  LVKLVKTSPELSESCSWFPESYVIYPTNLKTPVAPAQNGIQLPVSNSRTDEREFFLASYNRKKEDGEGNVWIAKSS 152
ratTTL    LVKLVKTSPELSESCSWFPESYVIHPTNLKTPVAPAQNGIQLPVSNSRTDEREFFLASYNRKKEDGEGNVWIAKSS 152
pigTTL    LVKLIKTSPELAESCTWFPESYVIYPTNLKTPVAPAQNGIHPPIHSSRTDEREFFLTSYNKKKEDGEGNVWIAKSS 152
cowTTL    LVKLIKTSPELAESCTWFPESYVIYPTNLKTPVAPAQDGIHPPLHSSRTDEREFFLASYNRKKEEGEGNVWIAKSS 152
          **** ****** *** ******** ************ **  *   ********** *** *** ************

humanTTL  AGAKGEGILISSEASELLDFIDNQGQVHVIQKYLEHPLLLEPGHRKFDIRSWVLVDHQYNIYLYREGVLRTASEPY 228
mouseTTL  AGAKGEGILISSEASELLDFIDSQGQVHVIQKYLERPLLLEPGHRKFDIRSWVLVDHQYNIYLYREGVLRTASEPY 228
ratTTL    AGAKGEGILISSEASELLDFIDNQGQVHVIQKYLEHPLLLEPGHRKFDIRSWVLVDHQYNIYLYREGVLRTASEPY 228
pigTTL    AGAKGEGILISSEATELLDFIDNQGQVHVIQKYLERPLLLEPGHRKFDIRSWVLVDHQFNIYLYREGVLRTASEPY 228
cowTTL    AGAKGEGILISSDATELLDFIDNQGQVHVIQKYLERPLLLEPGHRKFDIRSWVLVDHQFNIYLYREGVLRTASEPY 228
          ************ * ******* ************ ********************** *****************

humanTTL  HVDNFQDKTCHLTNHCIQKEYSKNYGKYEEGNEMFFKEFNQYLTSALNITLESSILLQIKHIIRNCLLSVEPAIST 304
mouseTTL  HVDNFQDKTCHLTNHCIQKEYSKNYGKYEEGNEMFFEEFNQYLTSALNITLESSILLQIKHIIRSCLMSVEPAIST 304
ratTTL    HVDNFQDKTCHLTNHCIQKEYSKNYGKYEEGNEMFFEEFNQYLTSALNITLENSILLQIKHIIRSCLMSVEPAIST 304
pigTTL    HTDNFQDKTCHLTNHCIQKEYSKNYGKYEEGNEMFFEEFNQYLTSALNITLESSILLQIKHIIRSCLLSVEPAIST 304
cowTTL    HMDNFQDKTCHLTNHCIQKEYSKNYGKYEEGNEMFFEAFNRYLTSALNITLESSILLQIKHIIRSCLMSVEPAIST 304
          * ********************************** ** *********** *********** ** ********

humanTTL  KHLPYQSFQLFGFDFMVDEELKVWLIEVNGAPACAQKLYAELCQGIVDIAISSVFPPPDVEQPQTQP--AAFIKL 377
mouseTTL  KHLPYQSFQLLGFDFMVDEELKVWLIEVNGAPACAQKLYAELCQGIVDIAISSVFPPPDTEQVPQQP--AAFVKL 377
ratTTL    KHLPYQSFQLLGFDFMVDEELKVWLIEVNGAPACAQKLYAELCQGIVDIAISSVFPPPDTEQVPQQP--AAFMKL 377
pigTTL    RHLPYQSFQLFGFDFMVDEDLKVWLIEVNGAPACAQKLYAELCQGIVDIAIASVFPPPDAEQQQQQPPPAAFIKL 379
cowTTL    KHLPYQSFQLFGFDFMVDEELKVWLIEVNGAPACAQKLYAELCQGIVDIAIASVFPPPDAEQQPPQP--ATFIKL 377
          ********* ******** ********************************** ******* **   **  * + **
```

c

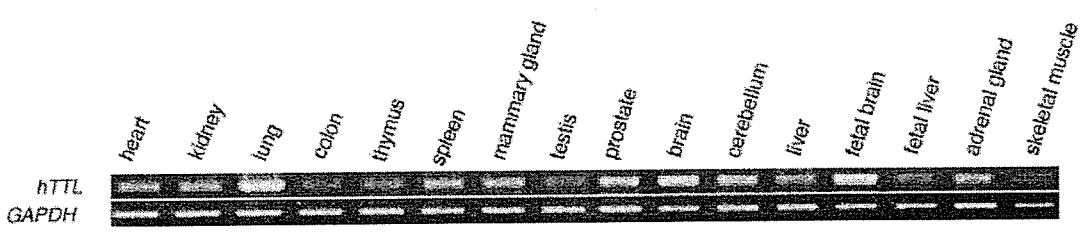

FIGURE 2

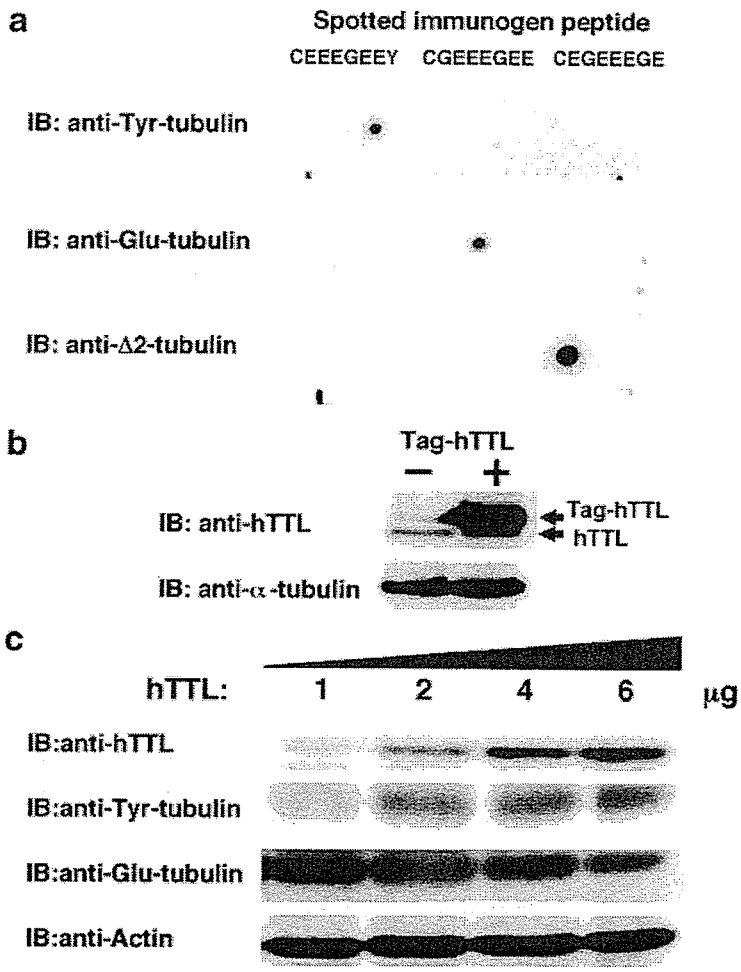

FIGURE 3 – hTTL has a tyrosination activity in mammalian cultured cells. (*a*) Specificity of antibodies. The indicated synthetic peptides were spotted on the filter and immunoblotted with the polyclonal anti-Tyr-tubulin (top), anti-Glu-tubulin (middle), or anti-Δ2-tubulin antibody (bottom). (*b*) Expression of FLAG-tagged hTTL. Whole-cell lysates prepared from COS7 cells transfected with the empty plasmid or with the expression plasmid for FLAG-tagged hTTL were subjected to immunoblotting with the anti-hTTL antibody (top). The expression level of α-tubulin was examined to ensure equal loading (bottom). (*c*) The exogenously expressed hTTL has a catalytic activity. HEK293T cells were transfected with increasing amounts of the hTTL expression plasmid. Forty-eight hours after transfection, whole-cell lysates were prepared and immunoblotted with the indicated antibodies. The expression level of actin is included as a loading control (bottom).

cells with 1 nM BMP2 or 5 μM RA induced remarkable morphologic differentiation by day 8. The hTTL protein level was increased after day 2 and peaked on day 6 in the former and on day 3 in the latter. Thereafter, it appeared to be decreased. Thus, hTTL was induced during induction of neuronal differentiation in NBL cells.

Expression of hTTL mRNA in primary neuroblastomas

To evaluate the clinical significance of *hTTL*, we examined the expression of *hTTL* mRNA in 16 favorable (stage 1, high expression of *TrkA* and a single copy of *MYCN*) and 16 unfavorable (stage 3 or 4, low expression of *TrkA* and amplification of *MYCN*) NBLs using semiquantitative RT-PCR. As shown in Figure 5(*a*), *hTTL* was preferentially expressed in favorable NBLs. Therefore, we next performed quantitative real-time RT-PCR to measure the levels of *hTTL* transcript in 74 primary NBLs. Table I shows the quantitative levels of *hTTL* mRNA expression (mean ± SEM) by age (< 1-year-old *vs.* ≥ 1-year-old), tumor stages (1 + 2 + 4s *vs.* 3 + 4), *TrkA* expression (low *vs.* high), *MYCN* gene copies (single *vs.* amplified), origin (adrenal gland *vs.* others), mass screening (tumors found by mass screening *vs.* sporadic tumors) and prognosis (alive *vs.* dead). High levels of *hTTL* expression were significantly associated with favorable stages ($p = 0.0069$), high *TrkA* expression ($p = 0.002$), a single copy of *MYCN* ($p < 0.00005$), tumors found by mass screening ($p = 0.0042$), origins other than adrenal gland ($p = 0.0042$) and a good prognosis ($p = 0.023$). *hTTL* expression was marginally associated with age. The log-rank test indicated that *hTTL* expression was associated with better survival ($p = 0.026$), which was also indicated in the Kaplan-Meier cumulative survival curves (Fig. 5*b*).

The univariate Cox regression was employed to examine the individual relationship of each variable to survival (Table II). Expression of *hTTL*, age, *MYCN* copy numbers and mass screening were found to be of prognostic importance, supporting the results of the log-rank test. However, since *hTTL* expression was highly associated with *MYCN*, mass screening and origin, multivariable Cox models were not fitted to assess the predictive importance of *hTTL* expression for survival after controlling these prognostic factors, suggesting that expression of *hTTL* was not an independent prognostic indicator.

FIGURE 2 – Genomic structure, alignment of amino acid sequence and mRNA expression of human *TTL*. (*a*) Genomic structure of *hTTL*. The *hTTL* gene that is mapped to 2q13 consists of 7 exons. Untranslated regions (open boxes) and coding regions (hatched boxes) are shown. Numbers indicate nucleotide position in human BAC clone *RP11-1124* (accession number AC012442). (*b*) Comparison of amino acid sequences among mammalian TTLs. The gaps produced by the alignment are indicated by a hyphen in the sequence. The conserved amino acid residues in TTLs are shown by asterisks below the alignment. (*c*) Tissue distribution of *hTTL* mRNA. The expression levels of *hTTL* mRNA in the indicated human tissues were examined by semiquantitative RT-PCR (top). *GAPDH* expression was also examined as an internal control (bottom).

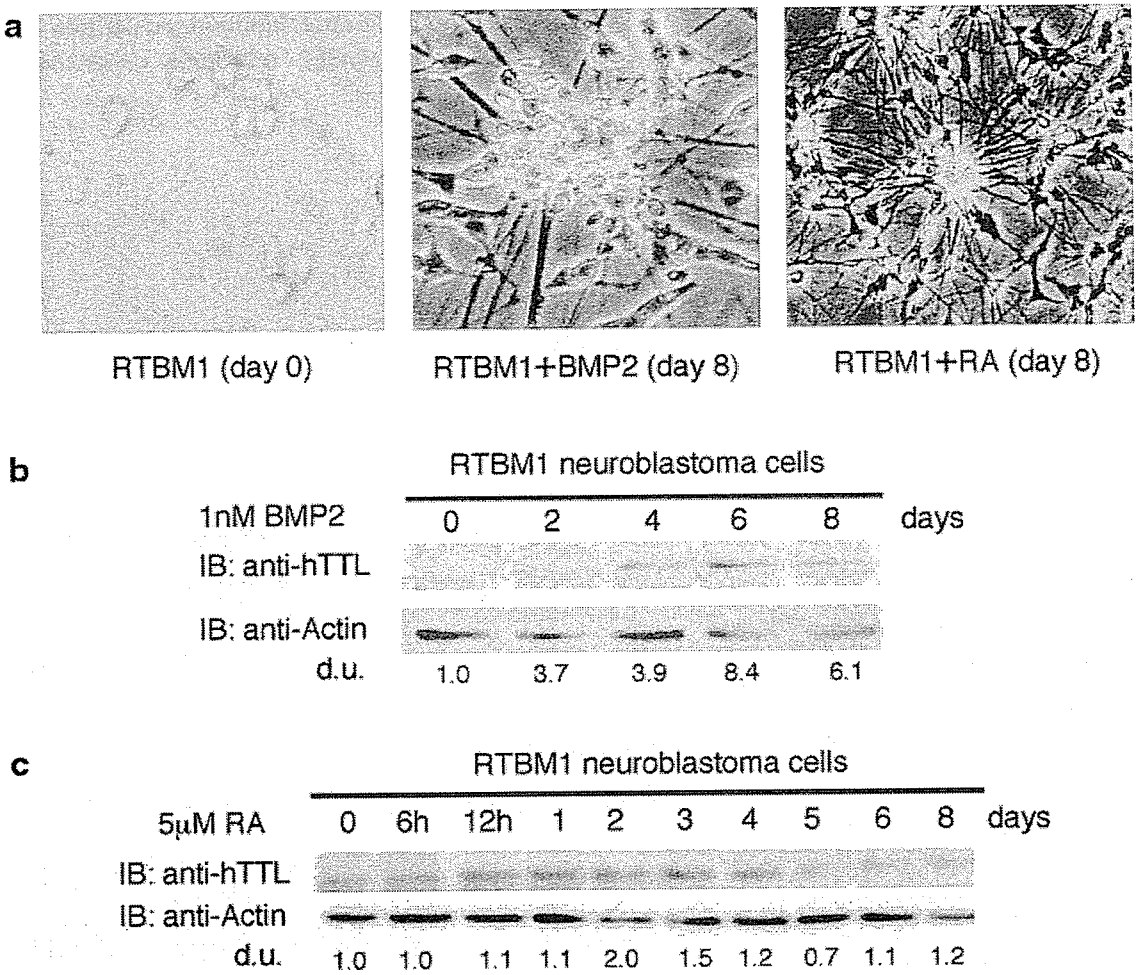

FIGURE 4 – TTL is induced during BMP2- and RA-mediated neuroblastoma differentiation. (*a*) BMP2- or RA-induced morphologic changes in RTBM1 neuroblastoma cells. RTBM1 cells were treated with BMP2 or RA at a final concentration of 1 nM or 5 μM, respectively, and maintained for 8 days. (*b*) Expression levels of hTTL are increased in response to BMP2. At the indicated time points after the treatment with BMP2 (at a final concentration of 1 nM), whole-cell lysates prepared from RTBM1 cells were subjected to immunoblotting with the antibody against hTTL (top). Actin protein levels were determined as a loading control (bottom). (*c*) Induction of hTTL in response to RA. RTBM1 cells were exposed to RA at a final concentration of 5 μM. Whole-cell lysates were prepared at the indicated time points after the treatment with RA and subjected to immunoblotting with the anti-hTTL (top) or with antiactin (bottom) antibody. d.u., arbitrary density units.

Immunohistochemistry

To determine the expression pattern of hTTL protein in primary NBLs, we performed immunohistochemical study for 6 favorable (stage 1 or 2 and a single copy of *MYCN*) and 4 unfavorable (stage 3 or 4 and amplified *MYCN*) NBLs. hTTL, Tyr-tubulin and Glu-tubulin were positively detected both in the cytoplasm of the neuroblastic cells and in the fine meshwork of neuropil of all 6 tumors with favorable histology (Shimada's classification) and a single copy of *MYCN* (Fig. 6*a–c*). In contrast, all 4 tumors with unfavorable histology and *MYCN* amplification were negative for Tyr-tubulin and Glu-tubulin, and only 1 tumor in this subset was positive for hTTL (Fig. 6*f–h*). Interestingly, all 10 NBL tumors were positive for Δ2-tubulin, but whose staining pattern was rather distinct in different subsets of the tumors. In the favorable tumors, Δ2-tubulin showed a localization similar to hTTL, Tyr-tubulin and Glu-tubulin and was detected in the cytoplasm and in the fine neuropil (Fig. 6*d*). On the other hand, Δ2-tubulin in the aggressive tumors was found only in the cytoplasm of neuroblastic cells, since they had no or a very limited capability of neuritic process production (*i.e.*, neuropil formation; Fig. 6*i*).

CD56 was detected in all 10 tumors, regardless of the histology and *MYCN* status (data not shown). TrkA was detected in all of 6 favorable tumors (Fig. 6*e*), but was negative in 3 of 4 aggressive tumors (Fig. 6*j*). It was noted that one unfavorable tumor with weakly positive trkA showed positive staining for TTL. Ki-67 staining revealed 10–20% and 60–70% positive cells in the favorable and the unfavorable tumors, respectively (data not shown).

DISCUSSION

In the present study, we have identified human ortholog of *tubulin tyrosine ligase* gene, which is highly conserved among the mammalian species. *hTTL* mRNA is ubiquitously expressed but rather preferential in both fetal and adult brains as well as in lung. The specific antibodies raised against hTTL, Tyr-tubulin, Glu-tubulin and Δ2-tubulin have confirmed the catalytic activity of

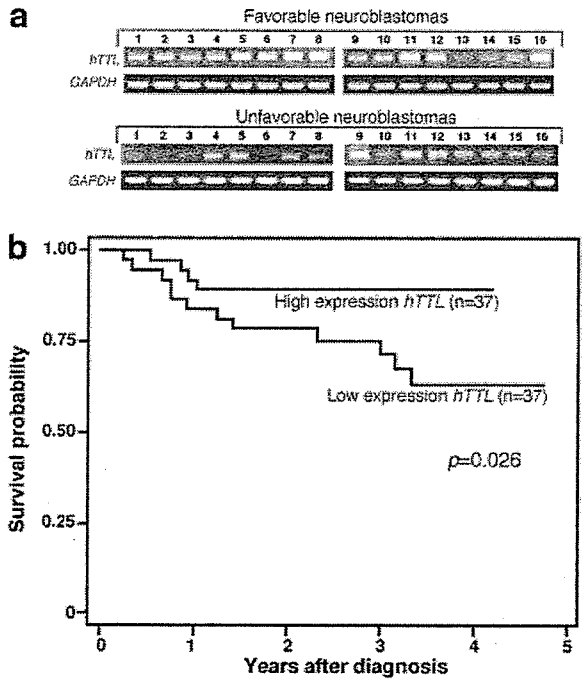

FIGURE 5 – Expression of *hTTL* mRNA is associated with unfavorable prognosis of neuroblastoma. (*a*) Total RNA was purified from the indicated favorable (top) and unfavorable NBL tissues (bottom) and subjected to semiquantitative RT-PCR. Sixteen favorable cases used in this study were classified as stage 1 NBL with a single copy *MYCN* as well as a high expression of *TrkA*. Sixteen unfavorable cases were in stages 3 and 4 NBL with *MYCN* amplification as well as a low *TrkA* expression. *GAPDH* expression was also examined as an internal control. (*b*) Association of *hTTL* mRNA expression levels with favorable prognosis of NBL. Total RNA was prepared from 74 NBL tissues, and *hTTL* mRNA levels were assayed by quantitative real-time RT-PCR as described in text. The values of *hTTL* mRNA were normalized by *GAPDH*. The survival of *hTTL* relatively high-expression group ($n = 37$) and *hTTL* low-expression group ($n = 37$) was compared using the Kaplan-Meier procedure.

TABLE I – RESULTS OF LOG-RANK TESTS FOR CONVENTIONAL PROGNOSTIC FACTORS AND EXPRESSION OF *hTTL* IN 74 PRIMARY NEUROBLASTOMAS

Variable	*n*	*hTTL* expression[1]	*p*-value
Age (year)			0.1
<1	43	117 ± 14	
≥1	31	77 ± 10	
Tumor stage			0.0069
1, 2, 4s	40	127 ± 14	
3, 4	34	69 ± 9	
TrkA expression			0.002
High	36	125 ± 17	
Low	38	77 ± 8	
MYCN			<0.00005
Single	52	123 ± 11	
Amplified	22	46 ± 9	
Mass screening			0.0042
+	37	128 ± 14	
–	37	72 ± 10	
Origin			0.0042
Adrenal gland	47	85 ± 11	
Others	27	127 ± 16	
Prognosis			0.023
Alive	58	113 ± 11	
Dead	16	54 ± 11	

[1]Mean ± SEM.

TABLE II – COX REGRESSION MODELS USING DICHOTOMOUS FACTORS OF AGE, *MYCN* AMPLIFICATION, MASS SCREENING, ORIGIN AND EXPRESSION OF *hTTL*

Factor	*p*-value	Hazard ratio (95% confidence interval)
hTTL expression (log)	0.024	0.64 (0.44, 0.94)
Age (> 1 *vs.* < 1 year)	0.005	5.04 (1.61, 15.8)
MYCN (1 copy *vs.* > 1 copy)	<0.0005	0.06 (0.017, 0.22)
Mass screening (+ *vs.* –)	0.004	0.05 (0.007, 0.38)
Origin (adrenal gland *vs.* others)	0.31	1.79 (0.58, 5.57)

hTTL encoded by the *hTTL* gene in the cells. Interestingly, hTTL is induced during neurite extension in RTBM1 NBL cells treated with BMP2 or RA, suggesting that hTTL expression is associated with neuronal differentiation in human NBL. Immunohistochemically, favorable NBLs are positive for hTTL, Tyr-tubulin, Glu-tubulin and Δ2-tubulin, whereas unfavorable tumors with *MYCN* amplification are positive only for Δ2-tubulin, suggesting that deregulation of tyrosination/detyrosination cycle contributes to malignant progression of NBL. This hypothesis has been further supported by a significant decrease of the levels of *hTTL* expression in the patients with poor prognosis.

The dynamics of microtubule regulates many cellular functions, including migration, motility, differentiation, cell division and cellular cap formation. Though posttranslational modifications of tubulin and their enzymatic regulation have long been studied, the precise mechanisms are still largely unknown. It is interesting that no orthologs of highly conserved mammalian TTL have so far been reported in *Caenorhabditis elegans*, *Drosophila melanogaster* and *Saccharomyces cerevisiae*, suggesting that the tyrosination/detyrosination cycle of tubulin may be related to evolution of the cellular functions, including neuronal differentiation. In newborn rats, TTL expression is found in skeletal muscle at high levels and is developmentally regulated by rapidly decreasing its level during early postnatal period.[31] It is interesting that both BMP2 and RA, which have increased levels of hTTL expression, function as regulators to induce differentiation during neural development.

The tyrosination/detyrosination of tubulin may be regulated by the activities of both TTL and tubulin carboxypeptidase (TCP). Until now, however, the *TCP* gene has never been identified in vertebrates, although biochemical TCP activity has been reported to be present in some subcellular fractions.[18] Tubulin is also posttranslationally modified by nitrotyrosination. Eiserich *et al.*[32] showed that free 3-nitrotyrosine (NO_2Tyr) is transported into mammalian cells and selectively incorporated into the Glu-tubulin posttranslationally, which is catalyzed by TTL. Cellular injury such as microtubule disorganization has consequently been induced. Kalisz *et al.*[33] also showed that nitrotyrosine can be incorporated into α-tubulin by *in vitro* assays. Those reports demonstrated that carboxypeptidase A is incapable of cleaving nitrotyrosine from the modified α-tubulin. On the other hand, Bisig *et al.*[34] reported that nitrotyrosinated tubulin is a good substrate of physiologic TCP, and that it has a similar capability to that of the tyrosinated tubulin to assemble into microtubules, suggesting that incorporation of nitrotyrosine is not injurious at least to dividing cells. Therefore, whether nitrotyrosinated tubulin is harmful or not is still controversial. Nevertheless, as increased nitrotyrosination is reported in Alzheimer's disease and amyotrophic lateral sclerosis,[35–37] the functional analysis of the role of hTTL and tubulin tyrosination/detyrosination cycle should be important for understanding the pathogenesis of these disease. The treatment of cells with methylmercury (MeHg) is also reported to induce perturbation of cellular activities associated with the tubulin/microtubule system by altering the status of tubulin tyrosination in the rat

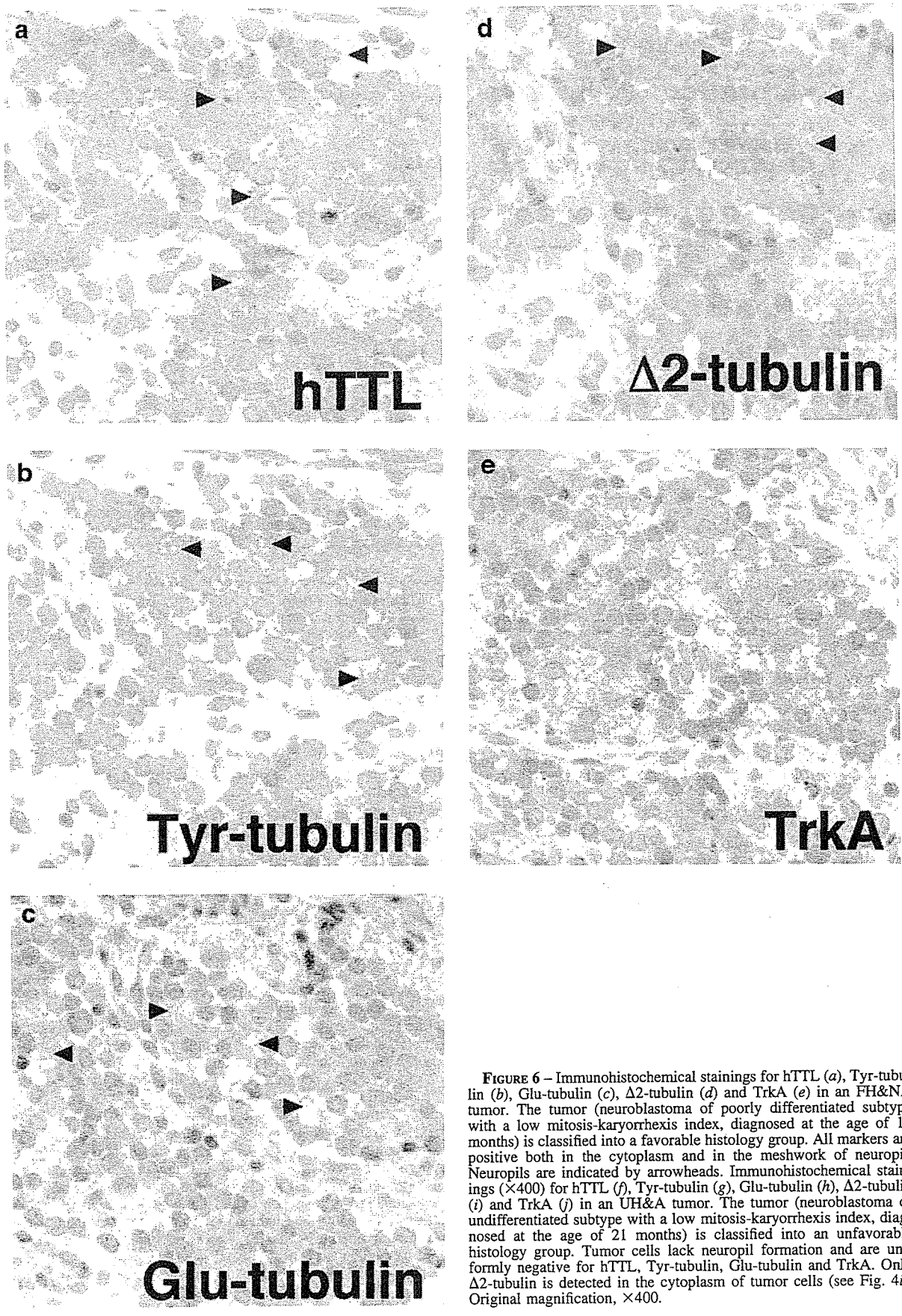

FIGURE 6 – Immunohistochemical stainings for hTTL (*a*), Tyr-tubulin (*b*), Glu-tubulin (*c*), Δ2-tubulin (*d*) and TrkA (*e*) in an FH&NA tumor. The tumor (neuroblastoma of poorly differentiated subtype with a low mitosis-karyorrhexis index, diagnosed at the age of 10 months) is classified into a favorable histology group. All markers are positive both in the cytoplasm and in the meshwork of neuropil. Neuropils are indicated by arrowheads. Immunohistochemical stainings (×400) for hTTL (*f*), Tyr-tubulin (*g*), Glu-tubulin (*h*), Δ2-tubulin (*i*) and TrkA (*j*) in an UH&A tumor. The tumor (neuroblastoma of undifferentiated subtype with a low mitosis-karyorrhexis index, diagnosed at the age of 21 months) is classified into an unfavorable histology group. Tumor cells lack neuropil formation and are uniformly negative for hTTL, Tyr-tubulin, Glu-tubulin and TrkA. Only Δ2-tubulin is detected in the cytoplasm of tumor cells (see Fig. 4*i*). Original magnification, ×400.

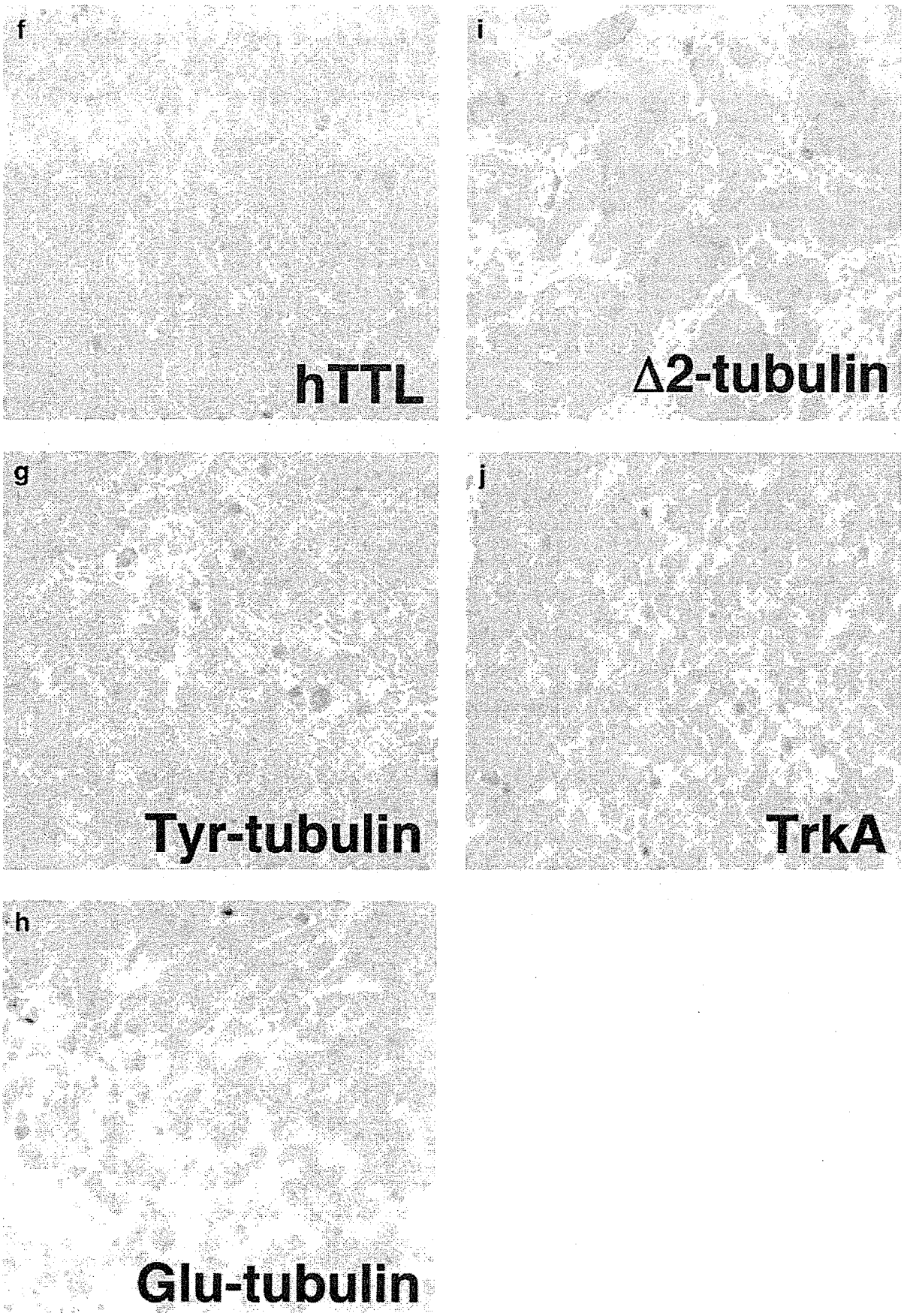

FIGURE 6 – (CONTINUED)

brain.[38] Therefore, many cellular stresses such as oxidative damage may trigger dysfunction of the tubulin/microtubule cytoskeletal system.

Our present study has shown that the decreases in Tyr-tubulin and Glu-tubulin are associated with relatively low levels of hTTL expression in unfavorable NBLs, which have lost a potency of neuronal differentiation and/or apoptosis. They are also correlated with decreased levels of TrkA, a high-affinity receptor for nerve growth factor, whose activation induces morphologic differentiation of NBL cells.[39] In addition, gradual upregulation of hTTL has been observed during induction of neuronal differentiation in RTBM1 cells treated with BMP2 or RA. These suggest that the induction of neuronal differentiation in NBL is accompanied with the activated tyrosination/detyrosination cycle regulated by increased level of hTTL enzyme, while the cycle is arrested by downregulation of hTTL in proliferating NBL cells, resulting in accumulation of Δ2-tubulin within the cells. Indeed, the expression levels of *hTTL* mRNA and Δ2-tubulin are significantly correlated with the prognosis of primary NBLs. This is consistent with the observation that TTL activity is lost, and conversely Δ2-tubulin is upregulated during the tumor cell growth.[19] Lafanechere *et al.*[19] have demonstrated by using mouse TTL null cells both *in vitro* and *in vivo* that mouse TTL activity is strongly decreased during tumor growth. Mas *et al.*[15] have also reported that, using rat *TTL* dominant negative mutant and an antisense cDNA of rat *TTL*, suppression of TTL activity induces 2- to 3-fold faster cell proliferation. Moreover, in human breast cancers, the accumulation of Glu-tubulin and Δ2-tubulin is correlated with poor prognosis by immunohistochemical approach.[28] It is noteworthy that our preliminary data using the microarray hybridized with total RNA obtained from 136 primary NBLs have shown that the gene with the highest score to predict prognosis of NBLs is α-tubulin (data not shown). Thus, the role of microtubule and its component, α-tubulin, is very important to define the biology as well as the aggressiveness of cancer cells.

In conclusion, we have identified a *human tubulin tyrosine ligase* gene and demonstrated its tissue distribution and correlation with neuronal differentiation. Since our data have suggested that the tyrosination cycle of α-tubulin is activated in differentiating NBLs but is inactivated in proliferating tumors, the cycle-related molecules including hTTL could be the targets for developing novel therapeutic strategies against advanced stages of NBL.

ACKNOWLEDGEMENTS.

The authors thank Shigeru Sakiyama for critical reading of the manuscript, Naoko Sugimitsu for preparing RNA, Yuki Nakamura for DNA sequencing, Yoshiaki Okamoto for instructing quantitative real-time RT-PCR and Aiko Morohashi and Natsue Akao for technical assistance. The authors also thank the following institutions for providing surgical samples: First Department of Surgery, Hokkaido University School of Medicine; Department of Pediatrics, National Sapporo Hospital; Department of Pediatric Surgery, Tohoku University School of Medicine; Department of Surgery, Gunma Children's Medical Center; Department of Pediatrics, Pediatric Surgery and General Surgery, Jichi Medical University; Department of Hematology and Oncology, Saitama Children's Medical Center; Department of Pediatrics, Juntendo University School of Medicine; Department of Surgery, Kiyose Metropolitan Children's Hospital; Department of Surgery and Pathology, Chiba Children's Hospital; Department of Pediatric Surgery, Chiba University School of Medicine; Department of Pediatric Surgery, Kimitsu Central Hospital; Department of Pediatric Surgery, Niigata University School of Medicine; Department of Pediatrics and Pediatric Surgery, Aichi Medical University; Department of Pediatrics, Kyoto Prefectural Medical University; Tumor Board, Hyogo Children's Hospital; Department of Pediatrics and Pediatric Surgery, Kagoshima University School of Medicine; Department of Pediatric Surgery, Showa University School of Medicine; Department of Pediatrics, Oita University School of Medicine; Department of Pediatric Surgery, Ohta General Hospital; Department of Pediatrics, Ichinomiya City Hospital; Department of Pediatric Surgery, Osaka City General Hospital; Department of Pediatrics, Nihon University School of Medicine; Itabashi Hospital; Department of Pediatric Surgery, University of Tsukuba School of Medicine.

REFERENCES

1. MacRae TH. Tubulin post-translational modifications: enzymes and their mechanisms of action. Eur J Biochem 1997;244:265–78.
2. Zambito AM, Wolff J. Palmitoylation of tubulin. Biochem Biophys Res Commun 1997;239:650–4.
3. Barra HS, Arce CA, Argarana CE. Posttranslational tyrosination/detyrosination of tubulin. Mol Neurobiol 1988;2:133–53.
4. Luduena RF. Multiple forms of tubulin: different gene products and covalent modifications. Int Rev Cytol 1998;178:207–75.
5. Barra HS, Unates LE, Sayavedra MS, Caputto R. Capacities for binding amino acids by tRNAs from rat brain and their changes during development. J Neurochem 1972;19:2289–97.
6. Barra HS, Rodriguez JA, Arce CA, Caputto R. A soluble preparation from rat brain that incorporates into its own proteins (14 C)arginine by a ribonuclease-sensitive system and (14 C)tyrosine by a ribonuclease-insensitive system. J Neurochem 1973;20:97–108.
7. Barra HS, Arce CA, Rodriguez JA, Caputto R. Incorporation of phenylalanine as a single unit into rat brain protein: reciprocal inhibition by phenylalanine and tyrosine of their respective incorporations. J Neurochem 1973;21:1241–51.
8. Barra HS, Arce CA, Rodriguez JA, Caputto R. Some common properties of the protein that incorporates tyrosine as a single unit and the microtubule proteins. Biochem Biophys Res Commun 1974;60:1384–90.
9. Arce CA, Rodriguez JA, Barra HS, Caputo R. Incorporation of L-tyrosine, L-phenylalanine and L-3,4-dihydroxyphenylalanine as single units into rat brain tubulin. Eur J Biochem 1975;59:145–9.
10. Argarana CE, Arce CA, Barra HS, Caputto R. *In vivo* incorporation of [14C]tyrosine into the C-terminal position of the alpha subunit of tubulin. Arch Biochem Biophys 1977;180:264–8.
11. Preston SF, Deanin GG, Hanson RK, Gordon MW. The phylogenetic distribution of tubulin:tyrosine ligase. J Mol Evol 1979;13:233–44.
12. Gabius HJ, Graupner G, Cramer F. Activity patterns of aminoacyl-tRNA synthetases, tRNA methylases, arginyltransferase and tubulin: tyrosine ligase during development and ageing of *Caenorhabditis elegans*. Eur J Biochem 1983;131:231–4.
13. Stieger J, Wyler T, Seebeck T. Partial purification and characterization of microtubular protein from *Trypanosoma brucei*. J Biol Chem 1984;259:4596–602.
14. Ersfeld K, Wehland J, Plessmann U, Dodemont H, Gerke V, Weber K. Characterization of the tubulin-tyrosine ligase. J Cell Biol 1993;120:725–32.
15. Mas CR, Arregui CO, Filiberti A, Argarana CE, Barra HS. Cloning of rat olfactory bulb tubulin tyrosine ligase cDNA: a dominant negative mutant and an antisense cDNA increase the proliferation rate of cells in culture. Neurochem Res 2002;27:1453–8.
16. Paturle-Lafanechere L, Edde B, Denoulet P, Van Dorsselaer A, Mazarguil H, Le Caer JP, Wehland J, Job D. Characterization of a major brain tubulin variant which cannot be tyrosinated. Biochemistry 1991;30:10523–8.
17. Paturle-Lafanechere L, Manier M, Trigault N, Pirollet F, Mazarguil H, Job D. Accumulation of delta 2-tubulin, a major tubulin variant that cannot be tyrosinated, in neuronal tissues and in stable microtubule assemblies. J Cell Sci 1994;107:1529–43.
18. Lafanechere L, Job D. The third tubulin pool. Neurochem Res 2000;25:11–8.
19. Lafanechere L, Courtay-Cahen C, Kawakami T, Jacrot M, Rudiger M, Wehland J, Job D, Margolis RL. Suppression of tubulin tyrosine ligase during tumor growth. J Cell Sci 1998;111:171–81.
20. Ohira M, Morohashi A, Inuzuka H, Shishikura T, Kawamoto T, Kageyama H, Nakamura Y, Isogai E, Takayasu H, Sakiyama S, Suzuki Y, Sugano S, Goto T, Sato S, Nakagawara A. Expression profiling and characterization of 4200 genes cloned from primary neuroblastomas: identification of 305 genes differentially expressed between favorable and unfavorable subsets. Oncogene 2003;22:5525–36.
21. Ohira M, Morohashi A, Nakamura Y, Isogai E, Furuya K, Hamano S, Machida T, Aoyama M, Fukumura M, Miyazaki K, Suzuki Y, Sugano S, Hirato J, Nakagawara A. Neuroblastoma oligo-capping cDNA

project: toward the understanding of the genesis and biology of neuroblastoma. Cancer Lett 2003;197:63–8.
22. Brodeur GM, Pritchard J, Berthold F, Carlsen NL, Castel V, Castelberry RP, De Bernardi B, Evans AE, Favrot M, Hedborg F, kaneko M, Kemshead J, Lampert F, Lee RE, Look AT, Pearson AD, Philip T, Roald B, Sawada T, Seeger RC, Thuchida Y, Voute PA. Revisions of the international criteria for neuroblastoma diagnosis, staging, and response to treatment. J Clin Oncol 1993;11:1466–77.
23. Kaneko M, Nishihira H, Mugishima H, Ohnuma N, Nakada K, Kawa K, Fukuzawa M, Suita S, Sera Y, Tsuchida Y. Stratification of treatment of stage 4 neuroblastoma patients based on N-myc amplification status: Study Group of Japan for Treatment of Advanced Neuroblastoma, Tokyo, Japan. Med Pediatr Oncol 1998;31:1–7.
24. Hishiki T, Nimura Y, Isogai E, Kondo K, Ichimiya S, Nakamura Y, Ozaki T, Sakiyama S, Hirose M, Seki N, Takahashi H, Ohnuma N, Tanabe M, Nakagawara A. Glial cell line-derived neurotrophic factor/neurturin-induced differentiation and its enhancement by retinoic acid in primary human neuroblastomas expressing c-Ret, GFR alpha-1, and GFR alpha-2. Cancer Res 1998;58:2158–65.
25. Chomczynski P, Sacchi N. Single-step method of RNA isolation by acid guanidinium thiocyanate-phenol-chloroform extraction. Anal Biochem 1987;162:156–9.
26. Shimada H, Ambros IM, Dehner LP, Hata J, Joshi VV, Roald B, Stram DO, Gerbing RB, Lukens JN, Matthay KK, Castleberry RP. The International Neuroblastoma Pathology Classification (the Shimada system). Cancer 1999;86:364–72.
27. Goto S, Umehara S, Gerbing RB, Stram DO, Brodeur GM, Seeger RC, Lukens JN, Matthay KK, Shimada H. Histopathology (International Neuroblastoma Pathology Classification) and MYCN status in patients with peripheral neuroblastic tumors: a report from the Children's Cancer Group. Cancer 2001;92:2699–708.
28. Mialhe A, Lafanechere L, Treilleux I, Peloux N, Dumontet C, Bremond A, Panh MH, Payan R, Wehland J, Margolis RL, Job D. Tubulin detyrosination is a frequent occurrence in breast cancers of poor prognosis. Cancer Res 2001;61:5024–7.
29. Iwasaki S, Hattori A, Sato M, Tsujimoto M, Kohno M. Characterization of the bone morphogenetic protein-2 as a neurotrophic factor: induction of neuronal differentiation of PC12 cells in the absence of mitogen-activated protein kinase activation. J Biol Chem 1996;271:17360–5.
30. Nakamura Y, Ozaki T, Koseki H, Nakagawara A, Sakiyama S. Accumulation of p27 KIP1 is associated with BMP2-induced growth arrest and neuronal differentiation of human neuroblastoma-derived cell lines. Biochem Biophys Res Commun 2003;307:206–13.
31. Arregui CO, Mas CR, Argarana CE, Barra HS. Tubulin tyrosine ligase: protein and mRNA expression in developing rat skeletal muscle. Dev Growth Differ 1997;39:167–78.
32. Eiserich JP, Estevez AG, Bamberg TV, Ye YZ, Chumley PH, Beckman JS, Freeman BA. Microtubule dysfunction by posttranslational nitrotyrosination of alpha-tubulin: a nitric oxide-dependent mechanism of cellular injury. Proc Natl Acad Sci USA 1999;96:6365–70.
33. Kalisz HM, Erck C, Plessmann U, Wehland J. Incorporation of nitrotyrosine into alpha-tubulin by recombinant mammalian tubulin-tyrosine ligase. Biochim Biophys Acta 2000;1481:131–8.
34. Bisig CG, Purro SA, Contin MA, Barra HS, Arce CA. Incorporation of 3-nitrotyrosine into the C-terminus of alpha-tubulin is reversible and not detrimental to dividing cells. Eur J Biochem 2002;269:5037–45.
35. Ischiropoulos H. Biological tyrosine nitration: a pathophysiological function of nitric oxide and reactive oxygen species. Arch Biochem Biophys 1998;3561–611.
36. Hensley K, Maidt ML, Yu Z, Sang H, Markesbery WR, Floyd RA. Electrochemical analysis of protein nitrotyrosine and dityrosine in the Alzheimer brain indicates region-specific accumulation. J Neurosci 1998;18:8126–32.
37. Beal MF, Ferrante RJ, Browne SE, Matthews RT, Kowall NW, Brown RH Jr. Increased 3-nitrotyrosine in both sporadic and familial amyotrophic lateral sclerosis. Ann Neurol 1997;42:644–54.
38. Ishida Y, Ichimura T, Sumi H, Horigome T, Omata S. Methylmercury alters the tyrosination status of tubulin in the brains of acutely intoxicated rats. Toxicology 1997;122:171–81.
39. Nakagawara A, Arima-Nakagawara M, Scavarda NJ, Azar CG, Cantor AB, Brodeur GM. Association between high levels of expression of the TRK gene and favorable outcome in human neuroblastoma. N Engl J Med 1993;328:847–54.